Geophys. J. R. astr. Soc. (1980) 63, 117–148

Explosive volcanic eruptions – IV. The control of magma properties and conduit geometry on eruption column behaviour

Lionel Wilson *Lunar and Planetary Unit, Department of Environmental Sciences, University of Lancaster, Lancaster LA1 4YQ*

R. Stephen J. Sparks *Department of Earth Sciences, University of Cambridge, Cambridge CB2 3EW*

George P. L. Walker *Department of Geology, University of Auckland, Auckland, New Zealand*

Received 1980 January 16; in original form 1979 August 9

Summary. Plinian air-fall deposits and ignimbrites are the principal products of explosive eruptions of high viscosity magma. In this paper, the flow of gas/pyroclast dispersions and high viscosity magma through various magma chamber/conduit/vent geometries is considered. It is argued that after the first few minutes of an eruption magma fragmentation occurs at a shallow depth within the conduit system. Gas pressures at the fragmentation level are related to exsolved gas contents by consideration of the exsolution mechanism.

The sizes of blocks found near vents imply that gas velocities of 200 to 600 m s^{-1} commonly occur. These velocities are greater than the effective speed of sound in an erupting mixture (90–200 m s^{-1}) and the transition from subsonic to supersonic flow is identified as occurring at the depth at which the conduit has its minimum diameter. The range of values of this minimum diameter (~ 5 to ~ 100 m) is estimated from observed and theoretically deduced mass-eruption rates.

The energy and continuity equations are solved, taking account of friction effects, for numerous geometries during the evolution, by wall erosion, of a conduit. Conduit erosion ceases, near the surface, when an exit pressure of one atmosphere is reached. Eruption velocities are found to depend strongly on exsolved magma gas content and weakly on radius of conduit and friction effects. Assuming water as the main volatile phase, velocities of 400–600 m s^{-1} for plinian events imply magma water contents of 3–6 per cent by weight.

Three scenarios are presented of eruptions in which: (1) conduit radius increases but gas content remains constant; (2) conduit radius increases and gas content decreases with time; and (3) conduit radius remains fixed and gas content decreases. These models demonstrate that the reverse grading

commonly observed in plinian air-fall deposits is primarily a consequence of conduit erosion, which always results in increasing eruption intensity and eruption column height with time. The models also show that a decrease in gas content as deeper levels in a magma chamber are tapped or an increasing vent radius as conduit walls are eroded leads to the prediction of a progression from air-fall activity through ignimbrite formation to cessation of eruption and caldera collapse.

1 Introduction

Explosive volcanic eruptions of high viscosity magma form two principal products: plinian air-fall deposits and ignimbrite. These eruptions are associated with the formation of calderas due to the evacuation of large magma chambers. We have presented in previous papers models of several of the processes and stages in these eruptions (Walker, Wilson & Bowell 1971; Walker 1972; Sparks & Wilson 1976; Wilson 1976; Sparks, Wilson & Hulme 1978; Wilson *et al.* 1978). We have shown that the conditions in the vent determine the style of the activity. In particular, the vent radius, gas content and composition, gas velocity and degree of fragmentation were shown to control the eruption column height and the circumstances under which column collapse to generate pyroclastic flows could occur. In this paper we examine the influence of the composition and content of volatiles, the distribution of volatiles in the magma, the viscosity of the magma and the shape of the conduit on the conditions in the vent and thus on the style of the activity. The most common type of high viscosity magma is rhyolite and we will present our models using the physical properties of rhyolite. However, our models would apply to any other type of high viscosity magma, such as phonolite, trachyte and pantellerite. We follow the arguments of Smith (1979) that there is a viscosity barrier below which this type of plinian/ignimbrite volcanism is not possible, because the gas and liquid can separate too easily.

Recent work (Wilson 1976) on the spatial distribution of ejecta found in plinian pyroclastic fall deposits implies that the gas velocity which entrains the ejected clasts is 400–600 m s^{-1}, assuming the magmatic gas is water at near-atmospheric pressure in the vent. Calculations by McGetchin & Ullrich (1973) on the flow of gas/tephra mixtures in diatremes and by Pai, Hsu & O'Keefe (1978) on possible high-speed lunar eruptions also predict flow speeds of this order. These velocities are much greater than the speed of sound in the Earth's atmosphere (about 330 m s^{-1}) and are also greater than a critical velocity, analogous to the speed of sound, for the erupting fluid itself. Transitions from subsonic to supersonic flow can only occur under certain combinations of circumstances; this restriction has led Steinberg & Steinberg (1975) and Housley (1978) to propose that exit velocities in basaltic eruptions are limited to the acoustic velocity and is explored here in some detail.

We model the steady flow of gas and fragmented rhyolitic magma from a chamber through a conduit out to the atmosphere and investigate the possible flow patterns that can remain stable during the course of such eruptions. These models apply to those types of eruptions where there is a near-continuous discharge into the atmosphere and are developed in Sections 2–5. Section 6 deals with non-steady aspects of large eruptions and Section 7 applies these general models to three eruption scenarios and deals with the interpretation of the principal geological characteristics of plinian deposits and ignimbrites.

2 Background assumptions

Fig. 1 shows the basis of the geometric constraints which we shall apply. A magma chamber is located beneath the surface and an eruption is initiated by the formation of a fracture

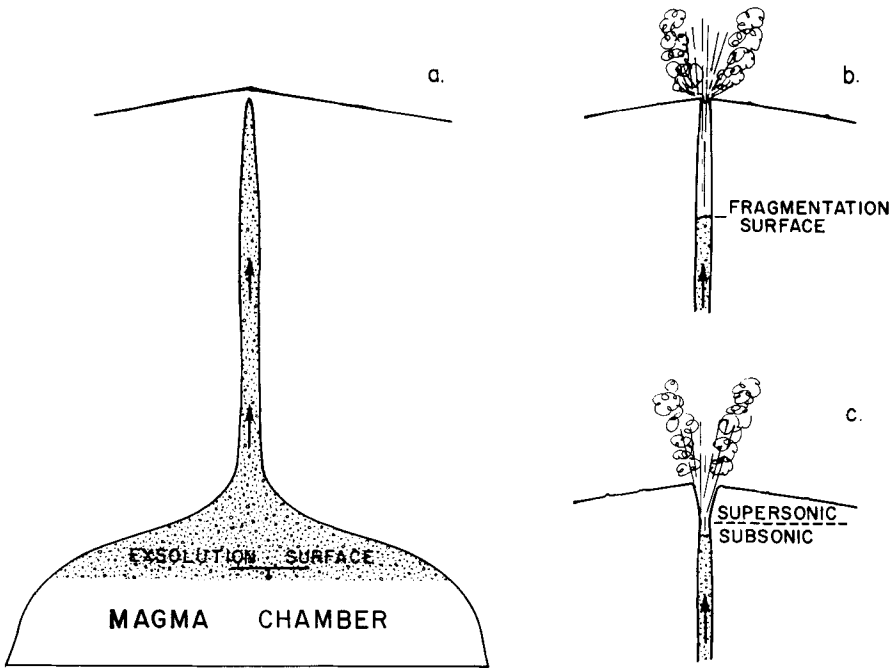

Figure 1. Development of eruption conditions. (a) Fracture propagating toward surface with gas exsolution beginning in upper part of magma; (b) fissure open to surface, magma fragmenting into gas and clasts in upper part of conduit, flow subsonic everywhere and exit pressure greater than atmospheric; (c) development of upper conduit and vent shape into flared structure permitting supersonic flow and exit pressure close to atmospheric.

(Fig. 1a) connecting the magma to the surface (Fig. 1b). The central position of the fracture in Fig. 1(a) is not critical: a ring fracture would be equally applicable. In Fig. 1(c) the eruption has been in progress for some time and has created a flared vent at the surface by erosion. The conduit has radius r_v at the surface (the vent radius). The diameters of calderas range from at least hundreds of metres to a few tens of kilometres, and are assumed to at least approximate the dimensions of magma chambers at depth. The volumes of plinian air-fall deposits and ignimbrites range from less than one to thousands of cubic kilometres and larger diameter calderas are generally associated with more voluminous eruptions. The vertical extent of caldera collapse is commonly from a few tens of metres to several hundred metres. These considerations are consistent with the commonly assumed shape of a chamber which has a bell-shaped or hemispherical section as shown in Fig. 1.

The chamber is connected to the surface by a conduit, the width of which must be small relative to that of the chamber. There are several geological and theoretical considerations which constrain the conduit shape. The conduit is likely to begin as a narrow fracture (Fig. 1a). Experience of basaltic eruptions which begin along fissures suggests that localization to form a 'central' vent is a common phenomenon. In explosive acid eruptions gas or magma flows through a narrow fissure in the initial stages and the widest part of the fissure offers the least frictional resistance to flow. High velocities result in the most rapid erosion of the conduit so the vent widens, further accentuating the flow at the widest point. A circular, central vent is the most favourable geometry to develop as it minimizes the ratio of surface-area to volume of flow. Although our model adopts the geometrical convenience of a circular vent, the results can be readily applied to a fissure eruption by replacing the vent radius by the half-width of the fissure.

The flaring of the vent shown in Fig. 1(c) is based on several considerations. Some vents, believed to be the sources of ignimbrites, are observed to converge downwards: (Almond 1971; Ekren & Byers 1976). Eichelberger & Koch (1979) propose that the vents associated with the formation of the Upper Bandelier Tuff must have been flared from the distribution and types of lithics in the tuff. Vent erosion is manifestly an important process during plinian and ignimbrite eruptions, as lithic fragments known to be derived from subsurface sources typically make up a significant proportion of these deposits (Kuno *et al.* 1964; Lirer *et al.* 1973; Bond & Sparks 1976; Bloomfield, Sanchez Rubio & Wilson 1977). As an example, the Fogo A plinian pumice deposit in the Azores (Walker & Croasdale 1971) contains 0.09 km^3 of lithic ejecta (14 wt per cent). If the magma source were at 5 km depth, a volume of solid rock equivalent to that of a cylindrical conduit with mean radius 78 m would be required to account for the ejecta. Vent erosion is considered to occur most efficiently near the surface since it is in this region that the conduit walls are most likely to consist of weak, imperfectly consolidated material.

Erupting material moving from a region of high pressure in a magma chamber to the Earth's surface can, in general, be divided into three zones. In a lower zone, the pressure is high enough that all the available volatiles are completely dissolved in the liquid magma. In a middle zone, the pressure is lower and some exsolution of volatiles can occur so that the magma consists of liquid and gas bubbles. In an upper zone, the pressure is so low that the magma has become disrupted into a mixture of pyroclasts and released gas. The boundary between the lower and middle zones may be called the exsolution surface and the boundary between the middle and upper zones the fragmentation surface.

The mean volume fraction of voids in pumice clasts and ash particles is typically 0.70–0.85, which implies that the magma disrupts when the volume fraction of gas approaches such values. The resulting fragments will be somewhat cooler than the original liquid, which will have already exsolved much of its dissolved gas during vesiculation. They may have gained some appreciable rigidity in this process. For the description of the gas/particle dispersion motion to the surface all that is important is that a single value can be assigned to the velocity of both gas and particle phases at any point within the flow. We will demonstrate that after magma fragmentation the pyroclasts, except the very largest fragments, do not have an appreciable terminal velocity through the gas.

We assume that the flow to the surface is a steady process. This is sufficiently accurate as long as the time rates of change are small compared to the spatial rates of change at any point. The geometry of the conduit and gas content of the magma inevitably change with time; therefore, strictly, an eruption is an unsteady process. However, we shall show that the transit time of material from the fragmentation level to the surface is of the order of 10 s in typical cases. The volume of magma erupted in such a short transit time is generally a very small fraction of the total magma volume eventually discharged. There is evidence that many of the magmas involved in explosive eruptions contain a few per cent volatiles by weight and that typically the volatile content will only vary by a factor of a few over the entire extent of a magma body (e.g. see Sommer 1977). Therefore, rapid fluctuations in volatile content will not occur on the time-scale of transit through the conduit.

We also assume that in the magma chamber and lower part of the conduit system the pressure is close to lithostatic. The wall rocks in these regions are generally hot, probably metamorphosed, and unlikely to be able to sustain large pressure differentials for long periods. In cases where the eruption is initiated by magma gas exsolution, the pressure in the erupting material will be somewhat greater than lithostatic, but the difference must certainly be less than the compressive strength of the walls, which is itself much less than the lithostatic pressure at depths greater than a few kilometres. Near the Earth's surface, vent and

upper conduit walls will behave in a more brittle fashion, withstanding the difference between the lithostatic pressure and the pressure in the erupting fluid. Wall bursting can occur if the fluid pressure drops below lithostatic pressure by an amount equal to the wall compressive strength.

Below the fragmentation level, the upward flow of the liquid/bubble mixture is limited by the high viscosity of the foam. The maximum rate of flow will occur when the pressure gradient is at a maximum. Since the pressure at great depths is constrained to be close to lithostatic, the maximum pressure gradient below the fragmentation surface will occur when the pressure at the fragmentation surface for a given conduit shape is equal to the local lithostatic pressure minus the wall rock compressive strength. Lower pressures would produce wall bursting.

Finally, we assume that the thermal contact between the vesiculating liquid or pyroclasts and gas is sufficiently good that a single temperature can be assigned to the mixture at all points. This is discussed by Sparks & Wilson (1976) and Sparks (1978) who argue that the efficiency of heat transfer between magma and gas will generally be high in eruptions of this type. Further evidence has emerged to support this assumption from studies of several plinian deposits: for example, the 1875 Askja plinian deposit contains at least 55 per cent by weight of sub-millimetre ejecta for which the thermal response time is less than a second (Sparks, Wilson & Sigurdsson 1980). Similarly, Walker (1980) has shown that in the very powerful plinian eruption of Taupo, New Zealand, in AD 131 over 80 per cent of the total mass consisted of material finer than 1/8 mm. Indeed it is emerging (Walker, G. P. L., unpublished data) that the degree of magma fragmentation increases in increasingly powerful plinian eruptions.

Furthermore, as a first approximation it is taken as adequate to keep the temperature of the mixture constant during the rise of the erupting fluid from the magma chamber. This latter assumption will require a small modification which is discussed later, owing to the fact that the *whole* system (gas plus liquid) expands adiabatically. However, in modelling *just* the expansion of the gas phase (the liquid being essentially incompressible) an isothermal model is most appropriate. The magma is a thermal reservoir which the gas continuously taps in transit to the surface.

3 Variables and equations

The quantities involved are as follows: let h be the vertical space coordinate measured positive upwards, and let u, P, ρ and σ be the velocity, pressure, bulk density and gas density, respectively, in the erupting fluid. The radius of the magma chamber or conduit through which flow is occurring is r and the friction factor specifying the drag at the wall is f. Let n be the weight fraction of the magma which consists of exsolved volatile phase and let R be the gas constant for the exsolved gas. The density of the liquid phase alone is σ_r and the absolute temperature of the mixture is T.

The basic equations are then:

$$-\frac{dP}{\rho} = g\,dh + u\,du + \frac{fu^2}{4r}dh \tag{1}$$

which expresses the conservation of energy; g is the acceleration due to gravity, and the last term represents frictional losses;

$$\dot{m} = \rho u \pi r^2 \tag{2}$$

which is the continuity equation where $\dot{m}$ is the mass rate of flow past a point, and can also be written:

$$\frac{d\rho}{\rho} + \frac{du}{u} + 2\frac{dr}{r} = 0. \tag{3}$$

The perfect gas law is an adequate approximation to the behaviour of both H_2O and CO_2 under the conditions encountered in these eruptions, and so the equation of state for the gas is:

$$P = \sigma RT \tag{4}$$

and the relationship between bulk, liquid and gas density is:

$$\frac{1}{\rho} = \frac{n}{\sigma} + \frac{(1-n)}{\sigma_r}. \tag{5}$$

After a little algebraic manipulation, these equations may be combined to give the following expressions:

$$\left(1 - \frac{u^2}{u_c^2}\right)\frac{du}{dh} = \left(\frac{u^2 f}{4r} + g\right)\frac{u}{u_c^2} - 2\frac{u}{r}\frac{dr}{dh} \tag{6}$$

$$\left(1 - \frac{u^2}{u_c^2}\right)\left(\frac{nRT}{P} + \frac{(1-n)}{\sigma_r}\right)\frac{dP}{dh} = 2\frac{u^2}{r}\frac{dr}{dh} - g - \frac{fu^2}{4r} \tag{7}$$

in which a new term u_c with dimensions of velocity has been introduced so that:

$$u_c = \sqrt{\frac{RT}{n}}\left(n + \frac{(1-n)P}{\sigma_r RT}\right). \tag{8}$$

Equations (6) and (7) represent the solution to the flow problem in the present case, where we shall present arguments which constrain the values of dP/dh and dr/dh.

The velocity u_c is closely related to the definition of the speed of sound in the magmatic fluid. The definition of the speed of sound, a, in a clean (i.e. particle-free) gas is:

$$a^2 = \frac{dP}{d\rho} \tag{9}$$

but ρ, the bulk density, is identical with σ, the gas density if no solids are present, and so equation (9) reduces to:

$$a^2 = \gamma RT \tag{10}$$

where γ is the ratio of the specific heats of the gas and it is assumed that the gas responds adiabatically to acoustic disturbances. In the present case we use equations (4) and (5) to relate ρ to P, and then find that equation (9) leads to:

$$a^2 = \frac{RT}{n}\left(n + \frac{(1-n)P}{\sigma_r RT}\right)^2 \tag{11}$$

so that a is identical to u_c as given by equation (8).

This identification of u_c with the speed of acoustic waves could only be exact if the non-gaseous part of the magma (i.e. pyroclasts after fragmentation or inter-bubble liquid before fragmentation) consisted of particles or liquid regions so small that they could undergo thermal interactions very quickly with the gas. In practice this would not be true for most fragments at acoustic frequencies even after magma disruption. However, we argued above that for the rates of gas pressure and density change envisaged in eruptions, the assumption of good thermal contact for most of the particles seems adequate (Sparks & Wilson 1976; Sparks 1978) and so u_c plays a role in the motion equivalent to that of the speed of sound in gases. A number of more detailed treatments of the flow of gas/solid dispersions exist (Soo 1961; Kliegel 1963; Soo 1967; Cole, Bowers & Hobbs 1969; Kieffer 1977). The present treatment is similar to those of Kliegel and Cole *et al.*, but differs in that the relative velocities of the particles and gas are negligible and a constant temperature is assumed. Cole *et al.* derive a formula for the effective speed of sound in a gas/solid dispersion which differs from that given here, when the above assumptions are inserted, by less than 7 per cent for n less than 0.06 and P less than 200 bars (the ranges of interest).

A singularity arises in equations (6) and (7) when $u = u_c$; both du/dh and dP/dh will be infinite unless the right-hand sides of the equations vanish. This criterion is satisfied simultaneously for both equations when dr/dh has a limiting value denoted $(dr/dh)_L$:

$$\left(\frac{dr}{dh}\right)_L = \frac{rg}{2u_c^2} + \frac{f}{8}. \tag{12}$$

This equation defines a critical condition in the eruption of a magma. If the flow commences at low velocity ($u < u_c$) from some point in the conduit/chamber system, and equation (12) is never satisfied, then the flow velocity must always remain less than or equal to u_c (which, as equation (8) shows, varies with pressure in the flow).

If, however, the conduit geometry and values of the magma gas content and pressure are favourable, then at some point equation (12) may be satisfied and the velocity u_c may be exceeded. A transition from subsonic to supersonic flow occurs, exactly analogous to the same transition in a clean gas passing through a suitably shaped nozzle. Provided certain simple geometric constraints are satisfied, the flow can remain supersonic to the surface and a high velocity eruption can occur. Table 1 shows values of u_c as a function of magma gas content n and pressure P given by equation (8) for $n = 0.01$, 0.03 and 0.05 and $P = 1$, 10, 100, 300 and 1000 bars. These values cover the range expected for erupting materials within a few kilometres of the surface. Clearly, for eruptions in which velocities of 400 m s^{-1} or greater are apparently involved in the vent (Wilson 1976), one must have $u > u_c$ in the flow near the surface unless unrealistically high pressures are to be invoked. The geometric constraints on the transition process can be illustrated by recalling that, in general, we expect the velocity to increase as the flow approaches the surface. Then, using equation (6):

Table 1. Values of the acoustic velocity, u_c, (equation 8) in m s^{-1} for various combinations of ambient pressure, P, in bars and exsolved water content, n, given as a weight fraction.

P:	1	10	100	300	1000
n					
0.01	72.3	77.7	126.9	237.3	623.6
0.03	124.6	127.4	155.5	217.9	436.5
0.05	160.7	162.8	184.1	231.5	397.3

(i) if $u < u_c$, then $(1 - u^2/u_c^2) > 0$ and if we wish to maintain $du/dh > 0$, we need:

$$\left(\frac{u^2 f}{4r} + g\right)\frac{u}{u_c^2} - \frac{2u}{r}\frac{dr}{dh} > 0$$

i.e.

$$\frac{dr}{dh} < \frac{rg}{2u_c^2} + \frac{fu^2}{8u_c^2}. \tag{13}$$

This inequality is satisfied for all negative dr/dh and for positive dr/dh less than the limiting value $(dr/dh)_L$ given by equation (12).

(ii) If $u > u_c$, then $(1 - u^2/u_c^2) < 0$ and for $du/dh > 0$:

$$\frac{dr}{dh} > \frac{rg}{2u_c^2} + \frac{fu^2}{8u_c^2} \tag{14}$$

so that dr/dh must be always greater than $(dr/dh)_L$. Thus, a sufficiently rapidly diverging conduit is needed to satisfy equation (14), whereas equation (13) can be satisfied by a converging or slightly diverging conduit. As the flow approaches the surface, one expects u_c to decrease as the pressure falls. If the flow becomes supersonic at some point and if u remains greater than u_c all the way to the surface, then it follows that the conduit is required to become ever wider from this point to the surface. Consider the inequality (14): dr/dh is necessarily positive. Even if u remains only slightly greater than u_c, so that the first term on the right-hand side is nearly constant, the second term must increase as u_c decreases and r increases. Hence, any small widening of the conduit requires an increase in the rate of widening; if the flow is to remain supersonic, a shape flared towards the surface (Fig. 1b) is implied.

Before equations (6) to (8) can be solved, numerical values are required for the material properties T, R and σ_r and the friction factor f; also, relationships between the local pressure, P, exsolved gas content, n, and depth, D, must be established.

4 Physical constraints on variables

4.1 MATERIAL PROPERTIES

The temperatures of silicic magmas at depth are generally believed to range from 700 to 1000°C and depend on the gas phase composition and content (Tuttle & Bowen 1958; Holloway 1976), on the degree of crystallization and on the magma composition. We adopt a temperature of 850°C (i.e. 1123 K) in all calculations; we will demonstrate that the eruption velocity, u_v, is very nearly proportional to the square root of magma temperature, so that the results given can be readily modified to those appropriate to other temperatures.

We adopt a constant density of 2.3×10^3 kg m^{-3} for liquid rhyolite in our calculations; eruption velocity is very insensitive to the actual value used.

H_2O is widely assumed to be the principal volatile component in silicic magmas. However, the importance of CO_2 in these magmas has become increasingly evident (Holloway 1976). There are few data on the H_2O/CO_2 ratios in acid magmas. Sommer (1977) found that the rhyolitic magma which produced the air-fall part of the Upper Bandelier Tuff contained between 5 and 7 per cent volatiles before eruption, based on studies of glass inclusions in quartz phenocrysts. He also found the H_2O/CO_2 ratio to be approximately 9. Our basic models assume that the only gas phase is H_2O, but we include some estimates of the effect

of H_2O/CO_2 mixtures and pure CO_2. The principal effect of increasing the proportion of CO_2 is to modify the gas constant, R, and the relationships between P and n (CO_2 is poorly soluble in magma at moderate pressures). We use $R = 461$ J kg^{-1} K^{-1} for H_2O and $R = 189$ J kg^{-1} K^{-1} for CO_2.

4.2 WALL FRICTION

The dependence of the friction factor f on Reynolds number and wall roughness for fluid flow in pipes is well documented (Hughes & Brighton 1967; Schlicting 1968). The Reynolds number, Re, for flow in a conduit, defined as $2r\rho u/\eta$ (where η is the fluid viscosity), will change dramatically in the vicinity of the level of magma fragmentation. Before fragmentation, the relevant viscosity is that of the liquid phase, of the order 10^4 to 10^7 Pa s for a rhyolite (Shaw 1963); afterwards it is that of the gas phase, about 2×10^{-5} Pa s. For the eruption velocities and vent radii deduced in the following section, Reynolds numbers will be high ($> 10^{11}$) after magma disruption and f will depend solely on conduit wall roughness, defined as the ratio of wall irregularity size to conduit diameter. The mean size of wall irregularities is assumed to be comparable to the joint-spacing of wall rocks in the conduit, which probably falls in the range 10–100 cm. We shall show that conduit diameters must be of order 20–100 m for most cases; the calculated range of friction factors implied varies between 0.005 (the limiting value for a completely smooth pipe at $Re < 10^{15}$) and 0.02.

Prior to magma fragmentation, the high viscosity of the liquid will generally lead to low Renolds number flow with a high value of f. Under these circumstances we can put $f = 64/Re$ (Hughes & Brighton 1967). When mass eruption rates are high and magma viscosity is relatively low, the transition from low Reynolds number, laminar flow to turbulent flow can occur (at about $Re = 2000$) when the value of f given above for disrupted magma is appropriate. The general expression for f is here taken to be:

$$f = \frac{64}{Re} + f_0 \tag{15}$$

with $f_0 = 0.01$; substituting for the Reynolds number, equation (15) becomes:

$$f = \frac{32\eta}{r\rho u} + f_0. \tag{15a}$$

4.3 RELATIONSHIP BETWEEN n, P AND DEPTH

Consider a magma containing water as its volatile phase. Let the total water weight fraction be n'. The solubility of water in rhyolite is given (Shaw 1974) by:

$$n_d = s\sqrt{P} \tag{16}$$

where n_d is the weight fraction dissolved at pressure P and the constant s has the value 4.1×10^{-6} m N$^{-1/2}$ (i.e. $s = 0.0013$ if P is expressed in bars). At depths sufficiently great that n_d calculated from this formula is greater than n', all of the water remains in solution. Exsolution of gas begins at a depth D_e at which n_d is just equal to n'. If the local pressure is taken to be lithostatic at the relevant depths, as argued in the previous section, we have:

$$\sigma_{cr} g D_e = \left(\frac{n'}{s}\right)^2 - P_s \tag{17}$$

where σ_{cr} is the density of crustal rocks and P_s is the pressure at the Earth's surface. If we use $\sigma_{cr} = 2800\ \mathrm{kg\ m^{-3}}$, then D_e ranges from 10.6 km for $n' = 0.07$ (i.e. 7 wt per cent) through 3.4 km for $n' = 0.04$ to 211 m for $n' = 0.01$. At depths less than D_e gas bubbles nucleate and grow as the pressure falls. Sparks (1978) has calculated the diffusional growth of H_2O bubbles in supersaturated magma and has shown that the mean size of inter-bubble liquid regions is such that the gas pressure in the bubbles and the vapour pressure of the gas remaining dissolved in the magma can be maintained close to equilibrium by diffusion even on the short time-scale of an eruption. The exsolved gas fraction, n, is therefore just equal to $(n' - n_d)$ at depths between D_e and the fragmentation surface.

Field evidence demonstrates that magma disrupts as a froth in which bubbles have grown as the magma is decompressed. Gas bubbles are able to grow until they are closely packed, at which stage growth is severely inhibited for several reasons (Sparks 1978). First, the bubbles, when closely packed, inhibit one another's growth because high viscosity liquid must be forced between the thin and tortuous walls separating bubbles in order for them to expand further (see also Bennett 1974). Secondly, rapid exsolution of gas increases the magma viscosity (Shaw 1963). When the viscosity is greater than 10^7 Pa s (residual water content generally less than 1 per cent by weight) the viscous resistance to growth is such that expansion is retarded even when the supersaturation pressure is tens of bars or more. McBirney (1973) and Sparks (1978) discuss this mechanism in more detail.

The details of the fragmentation process are poorly understood. The magma may disrupt by the bursting of many bubbles over a small range of depths, in which case the gas pressure decreases relatively rapidly in the region of disruption and the flow velocity rises in such a way that equations (6) to (8) apply. Some energy losses will occur due to the disruption process itself, but these are assumed to be minor. Rhyolitic magma which has exsolved volatiles is substantially undercooled and experimental data indicate that such melts may gain appreciable rigidity (Taniguchi 1974) and will certainly have high viscosity ($> 10^7$ Pa s). The shear stresses in the accelerating flow may become large enough to exceed the short-term tensile strength of the magma and contribute to disruption. The common occurrence of 'tube pumice' in which vesicles with near-circular cross-section are elongated by a very large factor in parallel directions is direct evidence for these large shear stresses.

Examination of pumices from many eruptions (Heiken 1972) shows that magma fragments when the volume fraction occupied by the gas, x, is close to 0.77 (pumices with this void fraction at atmospheric pressure have a bulk density of 500 kg $\mathrm{m^{-3}}$). It is easy to show that x and n (the exsolved gas weight fraction) are related by:

$$\left(\frac{n}{1-n}\right) = \left(\frac{x}{1-x}\right)\frac{P}{RT}\,\frac{1}{\sigma_r} \tag{18}$$

so that at the level where fragmentation occurs, we have:

$$n' = s\sqrt{P_F} + \frac{(x/1-x)P_F/RT}{\sigma_r + (x/1-x)P_F/RT}. \tag{19}$$

Given values for n', s, σ_r, R and T, this equation can be solved iteratively for P_F, the pressure at the fragmentation surface. If it is assumed that the magma volatile phase is CO_2, the problem is simpler since CO_2 is relatively insoluble at moderate pressures and the first term on the right-hand side of equation (19) can be neglected; the relevant value for R must, of course, be used in the second term. Fig. 2 shows the relationship between exsolved gas content, n, and pressure, P_F, for pure H_2O, pure CO_2 and two mixtures of these gases.

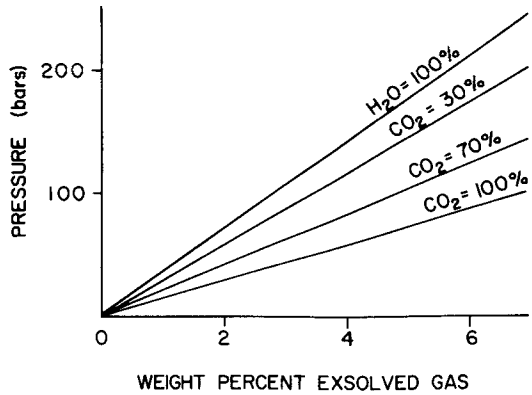

Figure 2. Variation of the gas pressure at the level where magma fragments with the weight per cent of total exsolved gases for four H_2O/CO_2 mixtures.

It was argued above that the pressure at the fragmentation surface should be less than the local lithostatic pressure by an amount equal to the tensile strength of the conduit walls, the value lying between zero and about 300 bars. We shall, in fact, present numerical solutions for these two extremes. The depth at which fragmentation takes place can be found as follows: Fig. 2 shows that for pure H_2O, $P_F = 211$ bars when $n = 0.05$; n' is then given by equation (19) as 0.069. If P_F is less than the local lithostatic pressure by a tensile strength of 300 bars, then the lithostatic pressure is $P_{LF} = 511$ bars and the fragmentation depth, D_F, is given by:

$$\sigma_{cr} g D_F = P_{LF} - P_s \tag{20}$$

so that $D_F = 1857$ m; Some other sets of values using the same tensile strength are: ($n = 0.03$, $n' = 0.044$, $P_{LF} = 424$ bars, $D_F = 1543$ m) and ($n = 0.01$, $n' = 0.0185$, $P_{LF} = 341$ bars, $D_F = 1236$ m). If the tensile strength is taken as zero instead of 300 bars, the fragmentation depths for these three cases become 768, 451 and 147 m, respectively. It is clear that fragmentation takes place within about 2 km of the Earth's surface unless total magma gas contents in excess of 7 per cent are invoked.

Solutions to equations (6) to (8) will now be presented, using various material properties and constraints developed above. We have devised a numerical integration scheme, programmed in FORTRAN IV, for use when no simplifying approximations to the equations can be made, but we also present simplified analytical solutions where these are adequate.

5 Numerical solutions

5.1 MOTION BELOW THE EXSOLUTION LEVEL

Here the problem is greatly simplified since we have no gas exsolution, i.e. $n = 0$. As a result, $\rho = \sigma_r$. We have also argued that the pressure, and more especially the pressure gradient, are close to lithostatic in this region, so we can put $dP = -\sigma_{cr} g\, dh$. Consider the continuity equation (3). If, for the moment, we imagine flow in a tube of constant radius r, we must have $dr = 0$. Since the liquid density ($\rho = \sigma_r$) is essentially constant we also have $d\rho = 0$, so it follows that $du = 0$ – the flow is at a constant 'terminal' velocity such that the buoyancy forces just balance viscous dissipation. If we substitute the general definition of f (equation 15a) into equation (1) together with $dP = -\sigma_{cr} g\, dh$ and $du = 0$, we find:

$$g(\sigma_{cr} - \sigma_r) = \frac{8\eta u}{r^2} + \frac{f_0 u^2 \sigma_r}{4r} \tag{21}$$

which is quadratic in u, the solution being:

$$u = \left(\frac{16\eta}{f_0 \sigma_r r}\right)\left(\sqrt{1 + \frac{gr^3(\sigma_{cr} - \sigma_r) f_0 \sigma_r}{64\eta^2}} - 1\right). \tag{22}$$

In the commonest case of laminar flow, the second term on the right hand side of equation (21) can be neglected; equation (22) then reduces, as one would expect, to the simple solution obtained by inspection of equation (21):

$$u = \frac{g(\sigma_{cr} - \sigma_r) r^2}{8\eta}. \tag{23}$$

These equations for u are, of course, only exact as long as all the variables on the right hand side are fixed. Now σ_{cr} and g can safely be regarded as constant; σ_r and η will only change if the composition of the erupting material changes (and even then are unlikely to change significantly on the time-scale of magma motion through the conduit). However, r, the conduit radius, may easily vary with depth. If it does, the magma velocity, u, constantly changes in an attempt to satisfy equation (22) – we have checked this by using the general numerical program to solve some examples, both for small variations in conduit radius and for flow from a wide magma chamber into a narrow conduit. Thus, if r is taken to be the mean conduit radius, then u given by equation (22) is the mean upward velocity of the magma.

It is instructive to evaluate the mass eruption rate, $\dot{m}$, in the case when equation (23) applies; substituting the relevant density and the above expression for u into equation (2) we have:

$$\dot{m} = \frac{\pi r^4 \sigma_r (\sigma_{cr} - \sigma_r) g}{8\eta} \tag{24}$$

which emphasizes the relative roles of r and η in restricting the mass eruption rate at depths below that at which gas exsolution begins.

5.2 EVOLUTION OF CONDUIT SHAPE

There are few simplifying assumptions that can be made about the motion in the upper part of the conduit system and the vent. Numerical solutions of equations (6) to (8) in several test cases showed that in eruptions with high magma viscosity, low gas content and low mass eruption rate, the value of du/dh is much less than the value of $fu^2/4r$ in the region between the gas exsolution level and the magma fragmentation level, and the value of ρ is nearly constant in this region, so that equation (1) takes on a simpler form than usual. We have used this approximation where it is valid, but have otherwise used the completely general numerical program mentioned above to solve for u and P as a function of depth and conduit radius.

The constraints on the ways in which a conduit/vent system is likely to evolve with time can be illustrated by considering the onset of the eruption. We assume a crack or fissure system opens rapidly to some finite size of order 10 m. This may be the result, as noted earlier, of a hydraulic fracture approaching the surface, or the result of a tectonic event. Whichever is the case, the crack is most likely to open at depth before it opens at the surface: the stresses required to fracture surface rocks, of order 100 bars, are small compared to ambient pressures at depths greater than a few kilometres. A stress 'event' that began near

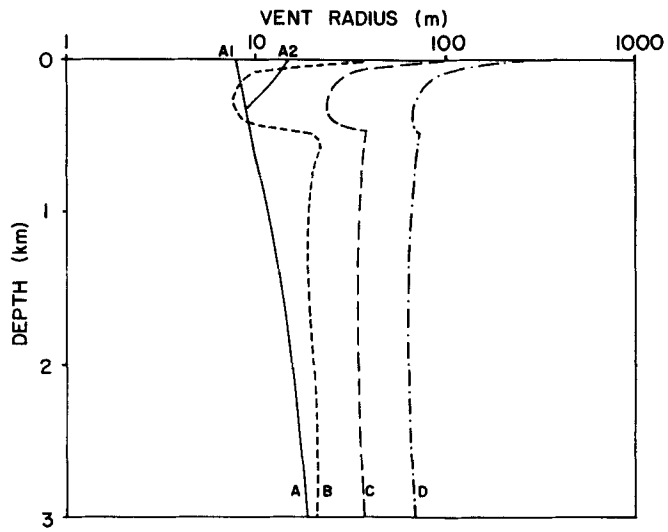

Figure 3. Variation of conduit and vent radius with depth below the surface for five models. For shapes B, C and D, the pressure is defined as lithostatic at all depths and the conduit radius and magma rise velocity (Fig. 4) are dictated by the pressure. For shapes A_1 and A_2 the conduit shape is chosen and the pressure and rise velocity are deduced.

the surface would be relieved by rock failure before it had attained a large enough amplitude to affect noticeably the rocks at greater depth.

As in the previous section we treat the case of a conduit with a circular section instead of an elongate crack, but the variations of flow velocity and pressure with depth are similar in the two cases. As an example consider a magma with viscosity 10^5 Pa s and total gas content 5 per cent by weight. Gas begins to exsolve from the liquid at a depth of 5.38 km (see equation 17). Below that depth, the steady state solution given by equation (22) for a constant crust–liquid density difference of 200 kg m^{-3} and a mass eruption rate of 10^7 kg s^{-1} has a liquid rise velocity of 1.73 m s^{-1} and a constant conduit radius of 26.6 m. We take as an arbitrary but plausible initial conduit shape that shown as curve A_1 in Fig. 3, which narrows linearly from 26.6 m at 5.38 km depth to 8 m at the surface. The profiles of rise velocity and pressure as a function of depth are shown as the curves labelled A_1 in Figs 4 and 5. The magma vesiculates progressively at depths between 5.38 and 1.6 km, where it fragments at a void fraction of 0.77. The flow velocity becomes sonic at depth 450 m and stays sonic until the surface where the eruption velocity is about 160 m s^{-1} and the exit pressure is about 56 bars.

An obvious consequence of the high exit pressure would be the rapid enlargement of the vent region by displacement of loose or weakly-cohesive materials; the curves labelled A_2 show the result of widening the vent region so that it expands from a radius of 8.6 m at a depth of 320 m to a radius of 15 m at the surface. The erupting gas/clast mixture makes the transition to supersonic flow at the 320 m depth level; the eruption velocity is about 275 m s^{-1} and the exit pressure is 8 bars. Clearly the exact final configuration is dependent largely on the strength of the near-surface layers.

A less obvious anomaly of this simple example is revealed by comparing the solution for conduit shape A with the solution, taken from the calculations of the previous section, in which the pressure is everywhere lithostatic: the curves labelled B in Figs 3, 4 and 5. Examination of the pressure values (Fig. 5) at depths around 1.6 km shows that the curve

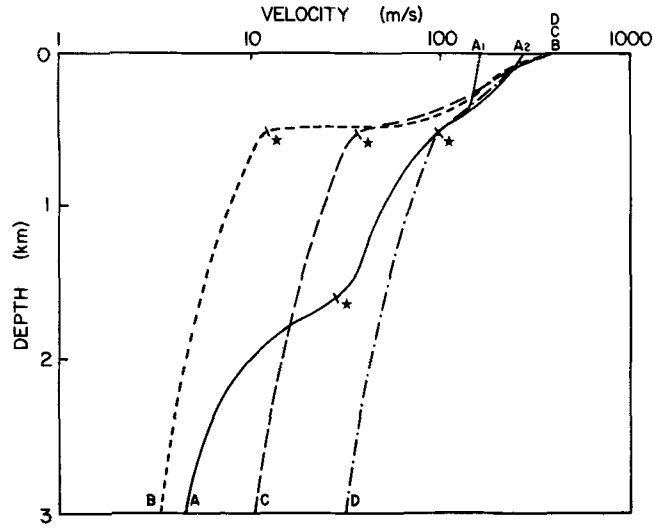

Figure 4. Variation of magma rise velocity with depth for the five models defined in the caption to Fig. 3. Above the levels of magma fragmentation (shown by ⋆) the velocity is that of the gas and small pyroclasts.

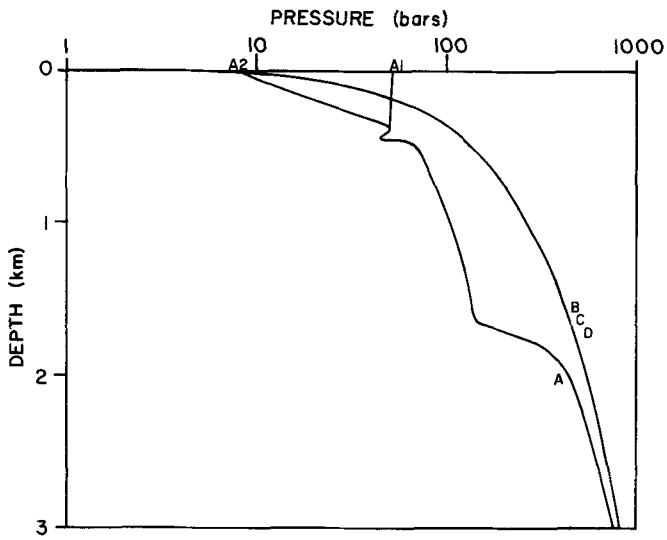

Figure 5. Variation of gas pressure with depth in the five model eruptions defined in the caption to Fig. 3. In cases B, C and D, the pressure is lithostatic everywhere.

A solution has pressures lower than the lithostatic values by as much as 280 bars. It seems inevitable that wall bursting would occur in this region very quickly, probably during the period of establishment of a steady flow regime in the open fissure. The time-scale for establishing a steady flow is clearly of the same order as the time taken for acoustic waves to propagate through the magma from the surface to the magma chamber. Equation (11) shows that acoustic wave velocities at pressures of the order of hundreds of bars in magmas with exsolved water contents of a few per cent are of order 200 m s^{-1}, so that the time-scale to establish steady flow from a depth of 5 km is about 30 s. We predict, therefore, that on a

time-scale of about 1 min the conduit would evolve from a shape like that of curve A, Fig. 3, to a shape qualitatively similar to curve B.

5.3 SOLUTIONS FOR 1 BAR EXIT PRESSURE

We believe that in extended eruptions, the evolution of the flared vent geometry at the surface occurs relatively quickly; we present solutions here for this case, in which the exit pressure in the vent, P_v, is one bar and the pressure in the conduit system is close to lithostatic, the exact distribution being dictated by the arguments in Section 4.3.

The solutions to equations (6) to (8) that are of interest consist of the values of u_v, the eruption velocity in the vent, and r_v, the vent radius, as a function of η, n (or n'), σ_{cr}, σ_r and the minimum radius of the conduit. In practice, since it is the exsolution of gas near the surface that dominates the motion, the effects of large changes in the adopted values of σ_{cr} and σ_r are completely undetectable. It was argued in Section 5.1 that the size of the conduit at great depths, just above the magma chamber, was, together with the magma viscosity, the controlling influence on the mass eruption rate. Conversely, if $\dot{m}$ and η are chosen, then the values of r and u are fixed at depth by equations (22) and (24). Mass eruption rate is a useful quantity to use to characterize an eruption, since we have already shown elsewhere (Wilson *et al.* 1978) that volcanic cloud heights, which can be deduced from the spatial dispersal of pyroclasts near the vent (Wilson 1978), can be related directly to $\dot{m}$. When we tabulate solutions in terms of η and $\dot{m}$, we find that the values of u_v and r_v are very insensitive to η for a given value of $\dot{m}$. This is again due to the fact that most of the acceleration of the eruption products by gas expansion occurs after the magma fragments; the second term on the right hand side of equation (15a) is then completely dominant at the expense of the term containing η. Thus we can present results as graphs of u_v and r_v as a function of $\dot{m}$ for several values of n (or n'), for each of the two assumptions about the location of the fragmentation level mentioned at the end of Section 4.3.

These results are summarized in Figs 6 and 7. u_v is only weakly dependent on $\dot{m}$ (Fig. 6) above $\dot{m} = 10^6$ kg s^{-1} and is controlled mainly by n (and hence n'). The velocities found by making the two extreme assumptions about the location of the fragmentation surface are similar at large values of $\dot{m}$ and differ by about 30 per cent at small values. Fig. 7 shows that r_v is much more strongly dependent on $\dot{m}$ than on n. Also, r_v is less sensitive than u_v to changing assumptions about the depth of fragmentation. This is simply due to the fact that, for a given mass eruption rate, $u_v r_v^2$ is a constant (see equation 2). Thus, a 20 per cent reduction in u_v would necessitate only a 10 per cent increase in r_v, approximately.

Mass eruption rates greater than 10^6 kg s^{-1} correspond to eruption cloud heights greater than about 10 km (Wilson *et al.* 1978), while $\dot{m} = 1.4 \times 10^9$ kg s^{-1} corresponds to a height of 55 km which is probably the greatest height that can ever be reached before column collapse to form pyroclastic flows occurs (Sparks & Wilson 1976). Thus, most large plinian eruptions have $\dot{m}$ in the range 10^6–10^9 kg s^{-1}, and over this range, Fig. 6 shows that u_v is almost entirely a function of n': the exit velocity of eruption products (and, consequently, the near-vent dispersal of ejecta) is much more strongly dependent on magma volatile content than, e.g. the local tectonic environment which may influence the vent size and geometry. Wilson (1976) deduced values of u_v in the range 400–550 m s^{-1} for 18 plinian and sub-plinian eruptions; these values correspond to total gas contents, n', in the range 5–7 wt per cent. If we make the assumption that the erupted magma is saturated with water, then the solubility function (equation 16) enables us to estimate the pressure in, and hence the approximate depth of origin of, the most gas-rich part of the magma as long as the pre-eruption pressure is close to lithostatic. Gas contents of 5 and 7 per cent would then correspond to depths of

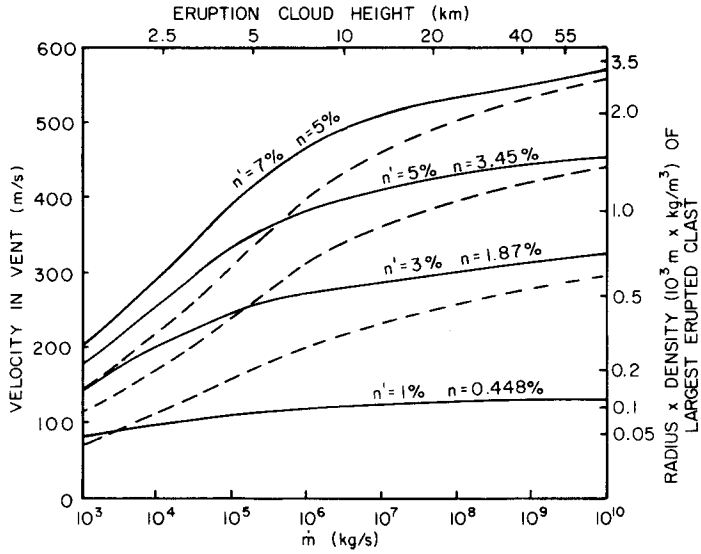

Figure 6. Solid lines: velocity of erupting gas/clast mixture in the vent as a function of mass eruption rate, $\dot{m}$, for four values of total magma water content n'; the weight per cent of water exsolved at fragmentation, n, is also given. Gas pressure is everywhere equal to lithostatic pressure and exit pressure in the vent is atmospheric. For the three cases $n' = 7$, 5 and 3 per cent, the broken lines show the result of assuming that the pressure at the fragmentation level is less than lithostatic by 300 bars. The scale at the top shows the eruption cloud heights corresponding to the mass eruption rates along the lower edge; the scale at the right shows the values of (clast radius x clast density) that correspond to the eruption velocities along the left side.

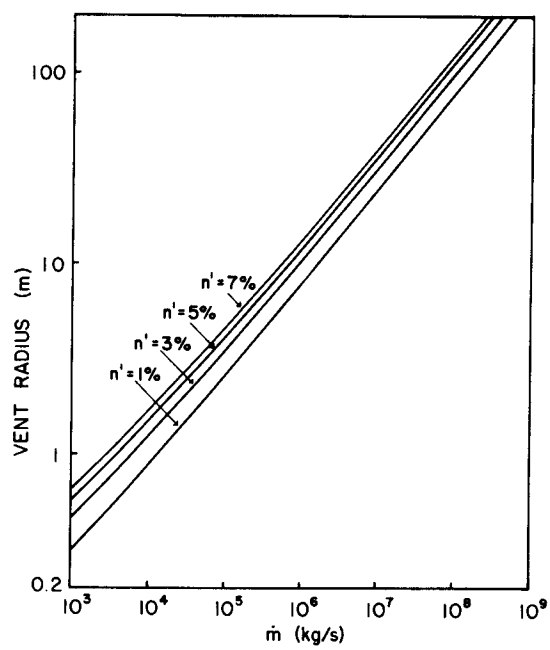

Figure 7. Variation of vent radius with mass eruption rate, $\dot{m}$, for the case where the pressure is lithostatic at all depths and the exit pressure in the vent is atmospheric. Curves are shown for four values of total magma water content, n': see Fig. 6 for corresponding values of n.

about 5 and 10 km respectively. Fig. 7 shows that for the range of gas contents 5–7 per cent, the implied radii of vent systems near the surface lie in the range 10–300 m.

5.4 ERUPTION CONDITIONS WITH EXIT PRESSURE GREATER THAN 1 BAR

It was shown in Section 5.2 that enlargement of the conduit into a vent at the surface could be limited by the finite strength of the near-surface materials. The commonest result of such limitation would be the prevention of a sub- to supersonic transition in the vent, as was the case for the profile A_1 in Figs 3, 4 and 5. The eruption velocity would then be limited to the local speed of sound in the gas/solid mixture, a circumstance proposed for lunar and terrestrial basaltic eruptions by Housley (1978).

We have calculated solutions for these conditions and find that the pressure in the vent is typically of order tens of bars while the eruption velocity is always less than 200 m s^{-1}. As in the case of 1 bar exit pressure, all three of the parameters eruption velocity, gas pressure and vent radius are functions of magma viscosity, mass eruption rate and magma gas content. Conveniently, eruption velocity depends mainly on gas content: Fig. 8. The finite spread of velocity shown for each value of total magma gas content, n', is due to the fact that velocity also increases with mass eruption rate and, weakly, with viscosity. Fig. 9 shows that vent radius is most strongly correlated with mass eruption rate, and hence with the average diameter of the conduit at depth. Again, a spread of values is shown since there is also a weak dependence on both viscosity and n'. The gas pressure in the vent (Fig. 10) shows significant dependence on both n' and mass eruption rate and is very weakly dependent on magma viscosity.

There are two major differences between eruption conditions described in this section and those of Section 5.2 where the exit pressure was assumed to be 1 bar. First, as the erupting mixture leaves the vent, lateral spreading must occur to allow the gas to decompress to atmospheric pressure. The decompression releases energy and the vertical velocity increases in the process (there are, of course, also transient horizontal velocities during the decompression). The increase in vertical velocity means that the continuity equation can be satisfied with a smaller lateral expansion than would be needed if the vertical velocity stayed fixed. Second, Wilson (1976) pointed out that the size of the largest clast of a given density that could be transported to the surface was proportional to the product of the gas

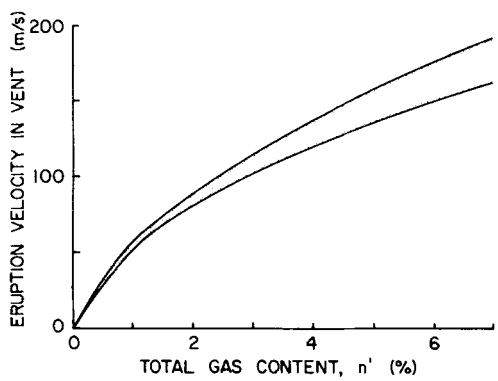

Figure 8. Variation of eruption velocity of gas and small clasts in the vent with total magma water content, n', for cases in which the velocity is limited to the acoustic velocity in the vent due to lack of outward flaring of the vent. The range of velocities at each gas content is the result of a small dependence on magma viscosity and mass eruption rate – see text, Section 5.4.

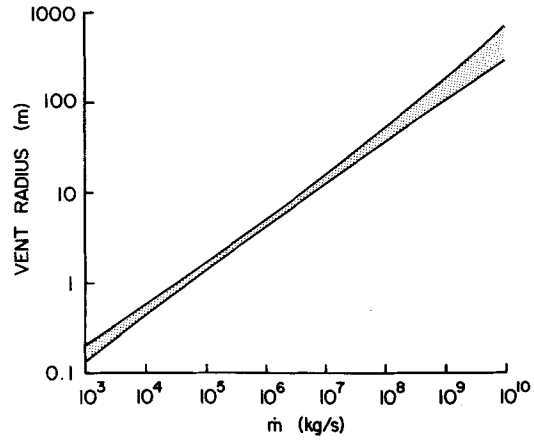

Figure 9. Variation of vent radius with mass eruption rate, $\dot{m}$, for the conditions given in the caption to Fig. 8. The spread of values for each value of $\dot{m}$ is due to a weak dependence on magma viscosity and gas content.

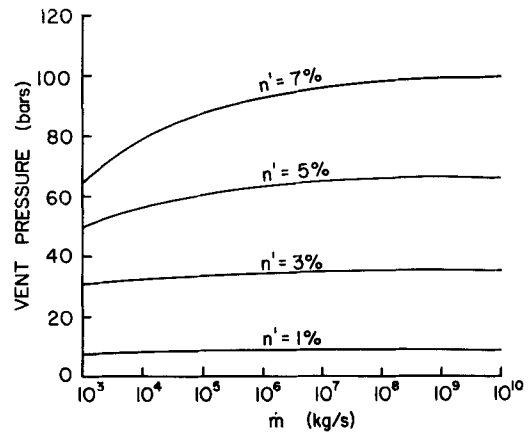

Figure 10. Gas pressure in the vent as a function of mass eruption rate, $\dot{m}$, and total magma water content, n', for the conditions given in the caption to Fig. 8.

density and the square of the eruption velocity in the vent (given a high particle Reynolds number) and this relationship was used to compute the products of clast radius and density shown on the right hand side of Fig. 6. The gas density in the vent is proportional to the local pressure, and so is greater in the case where the eruption velocity is limited to the sound speed. However, the eruption velocity is smaller in this case; comparison of Figs 6 and 8 shows that for mass eruption rates in excess of 10^6 kg s^{-1} the ratio of velocities is between 2 and 3. It happens that the excess gas density more than compensates for the reduced velocities in the transportation of clasts. The size of the largest clast that can be erupted near the vent is greater, during the early stages of the eruption when the exit velocity is limited by the vent geometry, by a factor which depends mainly on the magma gas content; the ratio varies from about 10 for $n' = 7$ per cent to about 3 for $n' = 1$ per cent.

5.5 EFFECTS OF PRESENCE OF CO_2

If more than one type of gas is present in the exsolved volatile phase, the equations presented earlier require slight modification: wherever the gas constant R appears it should

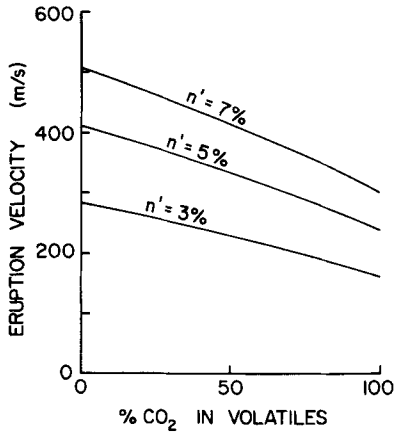

Figure 11. Variation of eruption velocity of gas and small clasts in the vent with proportion of CO_2 by weight in the exsolved volatiles (the other volatile being water) for eruptions in which the pressure is lithostatic at all depths and the exit pressure is atmospheric. Curves are given for three values of total magma volatile content, n'.

be replaced by the quantity R_0 defined by

$$R_0 = k_1R_1 + k_2R_2 + k_3R_3 + \ldots, \tag{25}$$

where k_1 is the weight fraction of the exsolved gas that has gas constant R_1, etc., and as many terms are included as there are types of gas present. Carbon dioxide is the most likely gas to be present in addition to water. Fig. 11 shows the variation of exit velocity, u_v, in the vent with weight proportion of CO_2 in the exsolved volatiles for constant values of mass eruption rate = 10^7 kg s^{-1} and an exit pressure of 1 bar. Three values of the total exsolved gas weight fraction at the fragmentation level are used, $n = 1.87$, 3.45 and 5 per cent, corresponding to total magma gas contents of $n' = 3$, 5 and 7 per cent, respectively, the values being chosen for comparison with the results shown in Fig. 6. Clearly, the presence of a large proportion of CO_2 (or any other high molecular weight gas) in the volatile phase significantly reduces the eruption velocity in the vent.

5.6 TEMPERATURE DURING MAGMA ASCENT

The assumption of isothermal gas expansion, made in solving the equations of motion, can now be justified. It is necessary to consider the energy balances during the acceleration of the magma. If we integrate the energy equation (1) without regard to the continuity equation (2) we can write

$$-\int_{P_i}^{P_f} \frac{dP}{\rho} = g\int_{h_i}^{h_f} dh + \int_{u_i}^{u_f} u\,du + \int_{h_i}^{h_f} \frac{f_0u^2}{4r}\,dh \tag{26}$$

where the subscripts i and f indicate initial and final values for the variables. If we use equation (5) to define ρ and evaluate most of the integrals, the above becomes:

$$-n\int_{P_i}^{P_f} \frac{dP}{\sigma} + \frac{(1-n)}{\sigma_r}(P_i - P_f) = g(h_f - h_i) + \tfrac{1}{2}u_f^2 - \tfrac{1}{2}u_i^2 + F \tag{27}$$

where F has been written for the last term of equation (26). We note that if pressures are close to lithostatic, $(P_i - P_f)$ can be replaced by $\sigma_{cr} g(h_f - h_i)$ and that σ_r is roughly equal to σ_{cr}; thus the second term on the left-hand side of the above equation is similar in value to the first term on the right-hand side. We have already shown that almost all of the increase in kinetic energy of the erupted material occurs in the region between the fragmentation level and the surface. We therefore identify P_i with P_F and take $P_f = 1$ bar. Our detailed numerical solutions have shown that frictional effects are small in the region above the fragmentation level and so the term F in equation (27) can be neglected; also u_i is very much less than u_f. We now have

$$-n\int_{P_i}^{P_f}\frac{dP}{\sigma} \approx \tfrac{1}{2}u_f^2. \tag{28}$$

The value of the integral depends on the assumption made about the mode of gas expansion. If the gas expands adiabatically from an initial temperature T, equal to the magma temperature, the result is

$$\tfrac{1}{2}u_f^2 \approx nRT\left(\frac{\gamma}{\gamma-1}\right)\left\{1-\left(\frac{P_f}{P_F}\right)^{\gamma-1/\gamma}\right\} \tag{29}$$

while if the expansion is isothermal at temperature T_c, the result is

$$\tfrac{1}{2}u_f^2 \approx nRT_c \ln\left(\frac{P_F}{P_f}\right). \tag{30}$$

The difference between these two expressions is the amount of energy that the non-gaseous part of the magma must supply, by cooling, to maintain the gas temperature as nearly as possible constant. Since some cooling must occur (the temperature could only remain exactly constant if the gas represented a vanishingly small fraction of the magma) it follows that T_c cannot be constant; if the magma temperature falls from its initial value T to a final value T_f, then T_c is well approximated by $\frac{1}{2}(T + T_f)$. If S is the magma specific heat we can then write:

$$S(T - T_f) = nR\left[\tfrac{1}{2}(T + T_f)\ln\left(\frac{P_F}{P_f}\right) - T\left(\frac{\gamma}{\gamma-1}\right)\left\{1-\left(\frac{P_f}{P_F}\right)^{\gamma-1/\gamma}\right\}\right]. \tag{31}$$

We have argued that n remains essentially constant above the fragmentation level; Fig. 2 can be used to select pairs of values of n and P_F and the above equation can be solved for the temperature decrease $(T - T_f)$. If $n = 5.1$ per cent, (corresponding to $n' = 7$ per cent) the decrease is 52 K; if $n = 1.87$ per cent (i.e. $n' = 3$ per cent) the value is 14 K. Even in the most extreme case, only 5 per cent of the thermal reservoir of the magma is utilized in producing the high eruption velocities, and our assumption of constant magma temperature is entirely adequate. Indeed, the above estimates of the amount of cooling are maxima, for they will be offset to some extent if viscous dissipation in the magma produces an appreciable temperature rise. Since T_f is only slightly different from T it follows that T_c in equation (30) is even more closely equal to T.

Equation (30), despite the many simplifying assumptions made in its derivation, gives quite good predictions of the eruption velocities when the exit pressure in the vent is atmospheric for all mass eruption rates greater than about 10^6 kg s^{-1}. Table 2 shows some sets of values of n', n, P_F and u_f. If the velocities are compared with those in Fig. 6 it is seen that the values from equation (30) correspond very closely to the accurately computed

Table 2. Sets of values of total magma water content, n', exsolved water content, n, gas pressure at the fragmentation level, P_F, and exit velocity in the vent, u_f, calculated from equation (30) for the case where the exit pressure in the vent is 1 bar.

n' (wt per cent)	n (wt per cent)	P_F (bars)	u_f (m s^{-1})
7	5.11	216	534
5	3.45	143	422
3	1.87	76	290
1	0.045	18	116

values for mass eruption rates between 10^7 and 3×10^7 kg s^{-1}. The form of equation (30) demonstrates that the eruption velocity approximated by u_f is proportional to the square root of T_c and hence to the square root of the magma temperature, T.

6 Time-dependent processes

6.1 ENTRAINMENT OF LARGE CLASTS

At the level of magma fragmentation, pumice clasts of a wide range of sizes will be produced. It is not guaranteed that the larger clasts or accidental lithics removed from the conduit walls will subsequently be transported to the surface by the erupting stream of gas and smaller clasts.

A particle of mean radius R_p and density σ_p will just be supported by the gas stream with density σ and velocity u if the particle weight is just balanced by the drag force of the gas, i.e.

$$\tfrac{4}{3}\pi R_p^3(\sigma_p - \sigma)g = \tfrac{1}{2}C_D\pi R_p^2\sigma u^2 \tag{32}$$

where, for motion at high Reynolds numbers, applicable to the cases studied here, the drag coefficient C_D takes on the value appropriate to cylindrical objects, about 1.2 (Walker *et al.* 1971). Fig. 12 shows the variation of the product σu^2 with depth corresponding to $n' = 5$ per cent, for mass eruption rates of 10^7, 10^8 and 10^9 kg s^{-1}. The pressure is taken to be lithostatic at all depths, so that these profiles correspond to those labelled B, C and D in Figs 3, 4 and 5. Using equation (32), the particle radius, R_p, for pumice clasts of density 1000 kg m^{-3} was found which corresponded to each value of σu^2 and these values are shown on the right hand side of Fig. 12.

For $\dot{m} = 10^9$ kg s^{-1}, the radius of the largest pumice clast that can be supported in the vent, 1.45 m, is smaller than the radius of the largest clast that can be supported immediately after fragmentation, 12.3 m. Clasts with radii greater than 12.3 m would accumulate at the fragmentation level, while those with radii less than 1.45 m would be transported out of the vent into the eruption column. Particles just smaller than 12.3 m radius would be able to leave the fragmentation region but would cease to be supported at a depth of about 60 m; clasts with radii between 12.3 m and 1.45 m would be trapped in decreasing size order between 60 m depth and the surface. A somewhat simpler pattern may be deduced from Fig. 12 for the case of $\dot{m} = 10^7$ kg s^{-1}. The largest clast that could be supported in the vent is bigger than the largest that could leave the fragmentation level (R_p = about 17 cm). Thus while all particles smaller than 17 cm radius would be transported out of the vent, all those larger would accumulate at a depth of just over 500 m. The general pattern of the diagrams for other gas contents is the same.

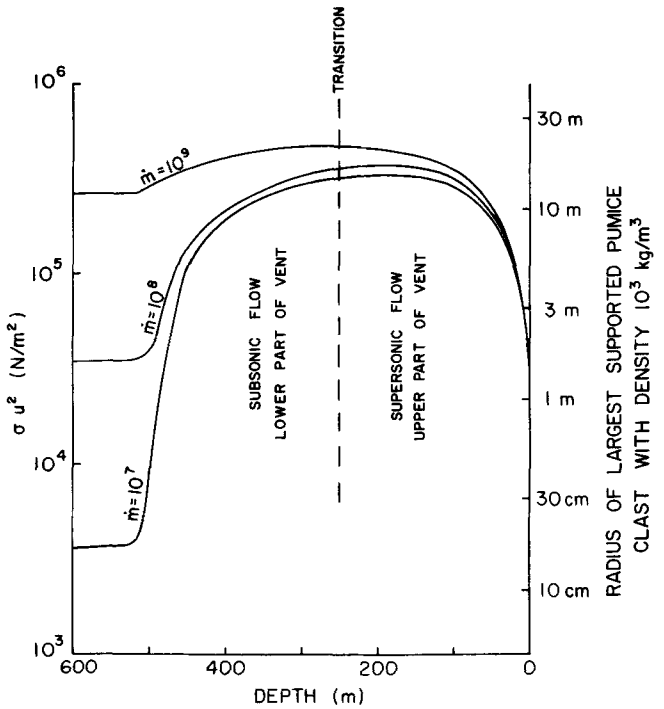

Figure 12. Variation of the quality σu^2 with depth in the vent region for three values of mass eruption rate, $\dot{m}$, for cases in which the pressure is lithostatic at all depths and the exit pressure is atmospheric. The sub- and supersonic flow regions are shown. The scale at the right edge shows the size of pumice clast which can just be supported at a given level.

The consequences of the accumulation of pumice clasts at various levels in the vent depends on their rate of accumulation. If large pumice clasts are removed by attrition faster than they accumulate, their presence represents only a minor perturbation to the solutions already presented. If they accumulate faster than they are removed, they must eventually become approximately stationary at some level in the system. Their presence has the same effect as a narrowing of the vent in their vicinity, and so their progressive accumulation acts in opposition to local conduit wall erosion. The result of such local narrowing is readily evaluated by suitable modifications to the numerical solution methods described earlier.

When flow conditions are supersonic in the upper part of the vent, narrowing of the vent leads to an increase in the local gas pressure and a decrease in flow velocity in such a way that the product σu^2 increases, thus tending to remove the obstructions. Consider an example with $\dot{m} = 10^8$ kg s^{-1} and $n' = 5$ per cent in which a number of 4 m radius lithic blocks, for which $\sigma u^2 = 2.2 \times 10^5$ N m^{-2}, have accumulated. Fig. 12 shows that they would begin to accumulate at a depth of about 50 m. As their numbers grew, the pressure would rise and the velocity would fall in the upper part of the vent until the support level coincided with the surface and the clasts were expelled from the edge of the eruption column, at which time a return to normal conditions would occur. Fig. 6 shows that the normal exit velocity for $\dot{m} = 10^8$ kg s^{-1}, $n' = 5$ per cent and 1 bar exit pressure would be about 425 m s^{-1}; Figs 8 and 10 show that the exit velocity could fall to about 150 m s^{-1} and the exit pressure could rise to about 65 bars before the exit velocity was in danger of becoming subsonic. If an exit velocity of 200 m s^{-1} is taken as an example, the gas density required to give $\sigma u^2 = 2.2 \times 10^5$ N m^{-2} is 5.5 kg m^{-3}, corresponding to a pressure of about 31 bars. The vent radius corresponding to $\dot{m} = 10^8$ kg s^{-1}, eruption velocity 200 m s^{-1} and exit pressure 31 bars

would be, using equations (2) and (5), 31.4 m, to be compared with the normal vent radius (Fig. 3) of 115 m. The difference in area corresponds to that occupied by the large clasts; if they were all large pumices of radius 10 m, the implied number in a layer one clast thick would be 122.

This example is idealized in that in practice a range of large clast sizes and densities would be present in a geometric arrangement more complicated than that used. All clasts smaller than the size used in the calculation would automatically be expelled, but any clasts larger than that size would remain in the vent. It is clear that in a real eruption, the exit pressure can only be exactly atmospheric if no clasts larger than the critical size that can just be supported in the vent by this pressure are produced: the limiting size/density products can be read from the scale on the right hand edge of Fig. 6. Otherwise, the population of clasts too large to be expelled from the vent with a vent exit pressure of 1 bar will cause a quasi-cyclic condition to be maintained in which the exit pressure fluctuates in response to the transient population of large clasts. The maximum pressure in the vent will be controlled by the size of the largest clasts that are produced in appreciable numbers, in line with the above calculation; the interval between occurrences of the maximum pressure will depend on the production rate of such clasts. Immediately after a phase of vent clearing, the exit pressure will fall to a value close to 1 bar and then begin to rise again.

Calculations have also been made of the effects of the accumulation of large clasts just above the fragmentation surface in the region of subsonic flow (Fig. 12). In this case, the localized constriction has the effect of increasing the flow velocity and decreasing the pressure in such a way that, as was the case for supersonic flow near the surface, the product σu^2 increases. Thus, the arrival of a very large clast may cause a rise in σu^2 sufficient to move smaller clasts, previously trapped in the same region, upward to a shallower depth. If constriction of the conduit increases sufficiently, the pressure may fall to the point where wall-bursting occurs. All small lithic fragments removed from the wall will be carried upward by the flow and, provided a relatively large proportion of small clasts are produced, the net effect will be to enlarge the conduit again.

To summarize, the effects of the presence of very large clasts are seen to be fluctuations, on a time-scale determined by the rate of production of such clasts, in the pressure and flow velocity profiles in the near-surface regions. The trend will be toward reduced pressures between the fragmentation level and the point where a supersonic transition occurs and raised pressures between the transition level and the surface, relative to the lithostatic profile. Eruption velocities will vary between maxima as given by Fig. 6 and minima which may approach the values given in Fig. 8, although the exact lower limits on velocity are determined by the sizes of the largest clasts produced.

All of the above examples have been calculated on the assumption that the mass flow rate of magma does not change as a result of the various perturbations. This seems to be the correct approach since, as shown in Section 5.1, the mass flow rate for a given viscosity is controlled almost entirely by the radius of the conduit at depths greater than about 2 km where the magma has exsolved little gas. The fluctuations in conditions described so far affect the deposition of erupted clasts near the vent, where inertial forces are important (Wilson 1976; Sparks & Wilson 1976; Blackburn 1977), but do not influence the properties of the upper, convective part of the eruption column which is controlled almost entirely by the mass eruption rate (Wilson *et al.* 1978).

6.2 CHANGES IN CONDUIT WIDTHS

Another geologically plausible cause of sudden changes in eruption conditions is a sudden partial closure of the conduit by faulting: Fig. 13(a). In order to investigate the importance

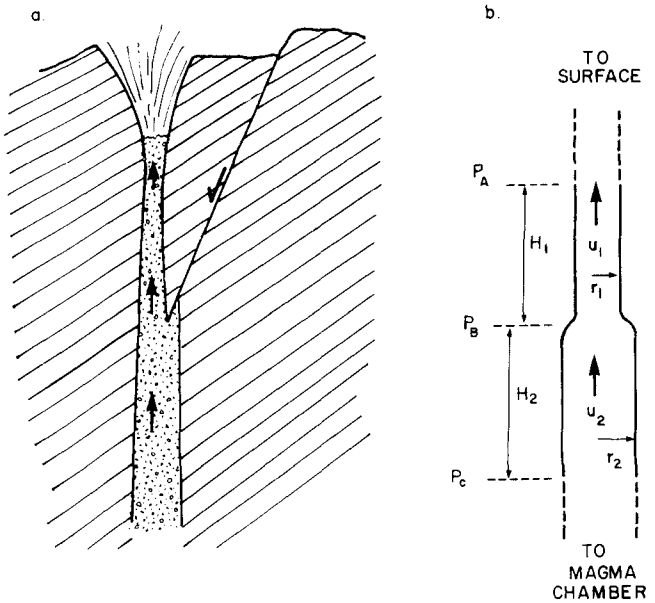

Figure 13. (a) Cartoon of major conduit constriction produced by downfaulting of crustal rocks; (b) idealized geometry used to simulate this system. P_A, P_B and P_C are pressures, u_1 and u_2 are velocities, r_1 and r_2 are tube radii and H_1 and H_2 are tube lengths.

of changes in conduit width at depth, we adopt the simple geometry of Fig. 13(b). A conduit is modelled as two adjoining circular cylinders with lengths H_1 and H_2 and radii r_1 and r_2, respectively. The velocity of rising magma is u_1 in the upper section and u_2 in the lower. To simplify the interpretation, we consider a range of depths where the amount of exsolved gas in the magma is negligible, so that the magma density is everywhere σ_r. The pressures at the extreme ends of the section and at the point of narrowing are P_A, P_C and P_B, respectively. We assume that P_A and P_C can be prescribed and that r_2 remains fixed; changes in r_1 and H_1 for fixed values of $(H_1 + H_2)$ then represent the effects of partial blocking of the upper part of the conduit by massive debris accumulation or by downward and inward faulting of crustal rocks. The system is described by the continuity equation:

$$\dot{m} = \sigma_r u_1 \pi r_1^2 = \sigma_r u_2 \pi r_2^2 \tag{33}$$

and the energy equations in the upper and lower sections, respectively:

$$P_B - P_A = g\sigma_r H_1 + \frac{8\eta u_1 H_1}{r_1^2} \tag{34}$$

$$P_C - P_B = g\sigma_r H_2 + \frac{8\eta u_2 H_2}{r_2^2}. \tag{35}$$

For simplicity, it has been assumed in equations (34) and (35) that the flow is laminar; suitable values of the variables used in the examples below can readily be chosen to ensure this. If the overall pressure gradient remains close to lithostatic, we have:

$$P_C - P_A = \sigma_{cr} g(H_1 + H_2). \tag{36}$$

Adding equations (34) and (35) and using equations (33) and (36) to eliminate u_2 and the pressures, we find for u_1:

$$(\sigma_{cr} - \sigma_r)g(H_1 + H_2) = 8\eta u_1 \left(\frac{H_1}{r_1^2} + \frac{H_2 r_1^2}{r_2^4}\right). \tag{37}$$

Once u_1 is obtained from this equation, (33) can be used to find u_2 and $\dot{m}$ and P_B can be found from either of equations (34) or (35). To correspond to earlier examples, we adopt $(\sigma_{cr} - \sigma_r) = 200$ kg m^{-3} and $\eta = 10^5$ Pa s; for an illustration we take $\sigma_{cr} = 2800$ kg m^{-3}, $P_A = 550$ bars (corresponding to a depth of about 2 km), $(H_1 + H_2) = 6$ km (which implies $P_C = 2198$ bars) and $r_2 = 30$ m. Fig. 14 shows the effect on the mass eruption rate, $\dot{m}$, of varying r_1 and H_1. The eruption rate through the undisturbed conduit is 1.622×10^7 kg s^{-1}. If, for example, the radius is narrowed from $r_2 = 30$ m to $r_1 = 15$ m, then the narrowing must extend over a vertical length, H_1, of at least 50 m before a significant change in the mass flow rate occurs; the order of magnitude of these values confirms that the assumptions made in calculating the examples of the consequences of large clast accumulation were adequate. If, however, r_1 becomes as small as 5 m, so that the conduit is almost closed off, then a vertical extent of blocking of as little as 5 m produces a significant change in the mass eruption rate.

The pressure, P_B, at the base of the narrowed region, increases as the mass eruption rate falls. In the present example, for which we assumed that pressures were everywhere lithostatic in the undisturbed conduit, P_B always takes on a value greater than the local lithostatic pressure. Examples of the excess pressures are shown in Fig. 14. The values show that an inward pressure of order tens of bars must be exerted on the conduit if narrowing is to be sufficient to change the mass eruption rate significantly. This circumstance could possibly happen in some eruptions as a result of the regional adjustment to the emptying of the magma chamber at depth. However, an actual positive pressure is not necessary: we argued

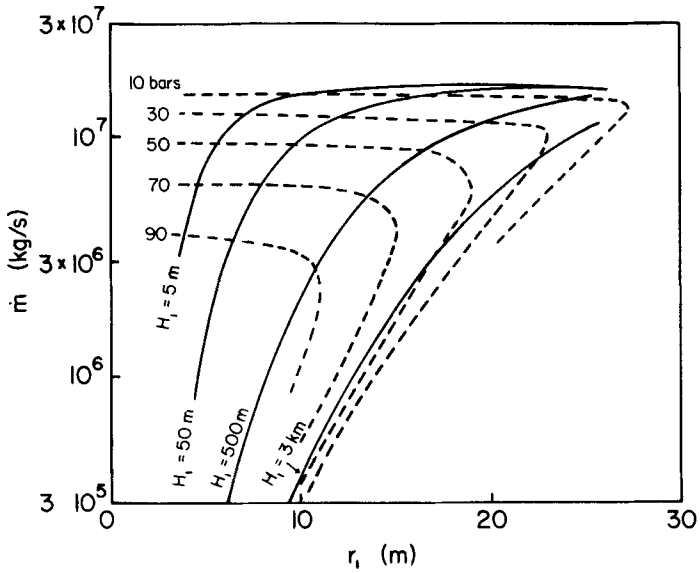

Figure 14. Variation of mass eruption rate, $\dot{m}$, with radius r_1 and vertical extent H_1 of constricted part of conduit system (see Fig. 13 for geometry). When there is no constriction, $\dot{m} = 1.622 \times 10^7$ kg s^{-1}. The broken lines show corresponding values of the excess pressure (in bars) (the amount greater than lithostatic) at the base of the constricted region.

in Section 5.3 that the consequence of the early stage development of the conduit shape would probably be a distribution of pressure in the erupting magma that was less than lithostatic by an amount equal to the tensile strength of the wall rocks, of order at least a few tens of bars. If this were the case, then a narrowing event of the kind illustrated here would simply correspond to a large-scale adjustment of the conduit walls and surrounding rocks to the tensile stresses acting across them.

7 Application of models to geological problems

7.1 SCENARIOS OF THREE MODEL ERUPTIONS

The two most important changes that take place during the course of large-scale explosive eruptions are in conduit shape and gas content. We now present three scenarios using the models outlined in the previous sections. Principally we wish to show the variations of column height and gas velocity that take place as a conduit erodes and as gas content decreases during the course of an eruption. In each scenario we assume a temperature of 1200 K, a lithostatic pressure gradient in the conduit and that the only volatile is water. Our models are thus most applicable to the eruption of silicic magmas.

The three scenarios are presented in Fig. 15 which shows the variations of column height and gas velocity with time. Wilson *et al.* (1978) and Settle (1978) have independently demonstrated that, in a convective eruption column, the maximum height of the column

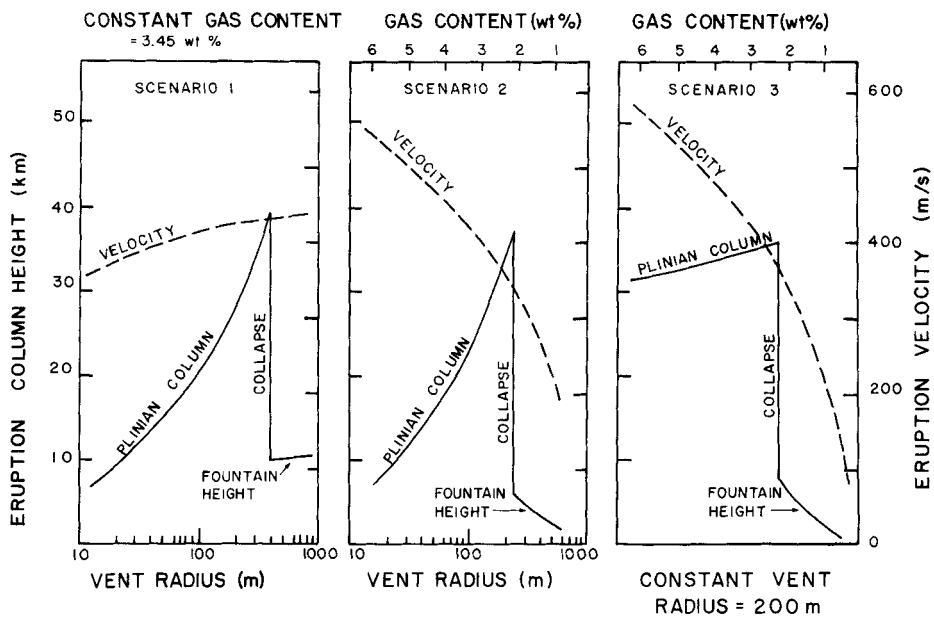

Figure 15. Scenarios of three model eruptions. In scenario 1, vent and conduit radius change with time while the exsolved water content remains fixed at 3.45 wt per cent. Eruption cloud height grows steadily with time until a sudden collapse occurs and a low ignimbrite-forming fountain is established. Eruption velocity in the vent increases slowly throughout the eruption. In scenario 2, vent radius increases with time (lower edge) and exsolved gas content decreases (upper edge). Column height variation with time is similar to scenario 1, though fountain height decreases with time after the collapse event. Eruption velocity decreases throughout the eruption due to the falling gas content. In scenario 3, vent radius is held constant and gas content decreases during the eruption. There is a much smaller variation in plinian cloud height. See text for detailed discussion.

is proportional to the fourth root of the heat release rate and hence to the fourth root of the mass eruption rate. Taking account of the specific heat of the magma and assuming that 70 per cent of the heat released by the erupted material in cooling through 900 K is used to drive convection (Wilson *et al.* 1978) we have:

$$H = 236.6\,\dot{m}^{1/4} \tag{38}$$

where H is the column height in metres and $\dot{m}$ is expressed in kg s^{-1}. We have also shown that certain combinations of vent radius, gas velocity and gas content produce convecting plinian columns while others produce column collapse to generate pyroclastic flows (Sparks & Wilson 1976; Wilson 1978; Sparks *et al.* 1978). From these studies we are also able to predict when column collapse will occur in the model eruptions and the fountain height of the collapsed column.

In scenario 1 (Fig. 15) the conduit erodes with time and the water content remains constant in the magma. As the surface vent widens the mass eruption rate increases resulting in a plinian eruption column which steadily grows in height. Eventually a vent radius is reached (390 m) where column collapse initiates. The height of the collapsing fountain thereafter stays steady at close to 10 km. The gas exit velocity shows a steady but gradual increase with time.

In scenario 2 (Fig. 15) the water content of the magma decreases from 6 to 1 wt per cent as the vent widens. A plinian eruption column again grows steadily with time and column collapse occurs at a vent radius of 230 m and a water content of 2.3 per cent. The gas velocity in this case diminishes with time and the height of the collapsing column fountain decreases with time. There is little difference in the rate of growth of the eruption column in scenarios 1 and 2 which graphically illustrates that eruption column height is only weakly controlled by gas content and is strongly dependent on vent radius. In scenario 3 the vent radius remains constant with time and only the water content in the magma decreases with time. We observe that in this case the column height stays almost constant although there is a very slight increase. The gas velocity decreases as the gas content decreases and once more column collapse occurs when the water content falls to less than 2.4 per cent.

The three scenarios represent a wide range of conditions but are simplified to the extent that it has been assumed that no events such as inward collapse of the conduit walls occur. The results of such events would be an abrupt re-setting of the mass eruption rate to a lower value with a consequent reduction of eruption cloud height. If column collapse had already occurred, re-instatement of the plinian eruption column would be possible if a large reduction in mass flow rate took place. The major features of the scenarios will be interpreted in the next sections in terms of the geological characteristics of plinian deposits and ignimbrites.

7.2 REVERSELY GRADED PLINIAN AIR-FALL DEPOSITS

Many examples of plinian air-fall deposits have been documented which show a noticeable reverse grading of clasts (Walker 1973). Examples of such grading include the Pompeii and Avellino pumice deposits of Vesuvius (Lirer *et al.* 1973), the Granadilla pumice deposit, Tenerife (Booth 1973), the Upper Toluca pumice deposit, Mexico (Bloomfield *et al.* 1977), the Minoan plinian deposit, Santorini (Bond & Sparks 1976), the 1875 plinian deposit of Askja, Iceland, the air-fall deposit of the Bishop Tuff, California and several sub-plinian deposits on Terceira in the Azores (Self 1976). In several cases the reverse grading is most pronounced at distances of 10–60 km and at these distances the maximum grain size at the top of the deposit can be up to two or three times larger than at the base. However, in the

cases of Santorini and Askja the reverse grading becomes only slight and even absent at localities close to the source ($\lesssim 5$ km), where the deposit becomes very coarse grained.

Possible causes of reverse grading have been discussed by Minakami (1950), Walker (1973), Lirer *et al.* (1973), Self (1976) and Duffield, Bacon & Roquemore (1979). Our models now demonstrate that a major cause of reverse grading in plinian deposits is vent widening caused by erosion. In scenario 1 gas exit velocity varies little with time and in scenarios 2 and 3 gas velocity decreases with time. Gas exit velocities are, however, important only in controlling the ejection and range of the very largest blocks which behave as ballistic ejecta (Wilson 1976). The absence of pronounced reverse grading in the near-vent coarse ejecta of Santorini and Askja is interpreted as evidence that the gas velocity did not vary greatly with time. However, in these same two deposits and in other plinian deposits there is pronounced reverse grading further away from the source: grain size typically ranges from 10 to 0.1 cm at these distances. The clasts which show the pronounced grading are too small to be transported ballistically, but are carried high into the eruption column before release. This suggests that their release height is controlled by the convective velocities within the main part of the plume, not by the initial gas exit velocity. As the column height increases the convective velocity at any given level also increases (Wilson, unpublished calculations) and particles of a given size are released at an increasing height.

Thus the simplest explanation of reverse grading in the 10–0.1 cm size range is that the release height of a particular grain size increases with time and hence the range downwind also increases. Other causes such as shift in wind direction and in wind speed may of course produce reverse grading in particular cases, but are hardly a plausible explanation for the common occurrence of this feature. Changes in wind regime should also produce just as many examples of normally graded as reversely graded deposits. The release height of these particles is controlled by the variation of the convective column velocity with height. They are released where the convective velocity becomes comparable with the terminal velocity of the particular clast. Convective velocities are only marginally related to gas exit velocities. They are in fact much more sensitive to the changes in the mass and energy flux (i.e. mass eruption rate) and therefore column height. Hence vent radius is of substantial importance in controlling convective velocities. The greater part of an eruption column consists of a convective plume in which the velocity at a given height is related to total column height, because both parameters are controlled by the total mass flux (Wilson *et al.* 1978). Reverse grading is thus evidence of increase in column height and mass flux but not necessarily gas exit velocity. Thus both scenarios 1 and 2 would produce reversely graded plinian deposits.

7.3 TRANSITION TO IGNIMBRITE FORMATION

Another characteristic of many eruption sequences is the eventual abrupt collapse of the eruption column to generate pyroclastic flows. Our present work suggests that collapse is an inevitable result of all scenarios where either the conduit wall erodes or gas content decreases to a sufficient extent. There are many examples of sequences where a plinian pumice fall deposit is overlain by ignimbrite (Sparks *et al.* 1978; Sparks & Wilson 1976) and the models provide a satisfactory explanation of the apparently sharp transition from one style of activity to another.

Sparks & Wilson (1976) in their Fig. 3 found that at certain critical combinations of vent radius, gas velocity and gas content, a transition occurs from column convection to column collapse. With the models developed here, gas velocity can be related to exsolved water content (Fig. 6) and the number of permutations of the critical conditions are consequently greatly reduced. Fig. 16 shows the combinations replotted in this way and the fields of

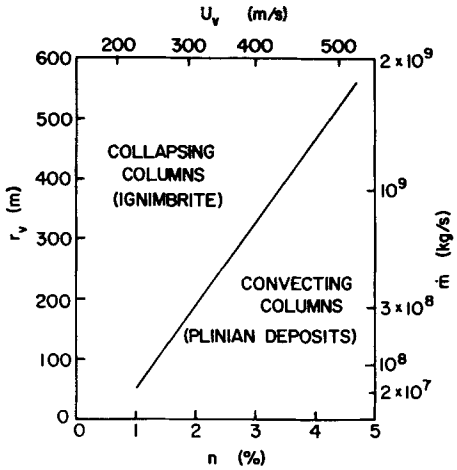

Figure 16. Combinations of vent radius, r_V, and exsolved water content, n, at which column collapse occurs. Mass eruption rates, $\dot{m}$, corresponding to the values of r_V are shown at the right edge, while values of eruption velocity, u_V, corresponding to values of n are shown at the top. The pairs of values can be used interchangeably since u_V depends much more strongly on n than on any other variable (Fig. 6), while $\dot{m}$ is largely a function of r_V (Fig. 7). The regions corresponding to convecting columns and collapsed columns are shown.

convecting plinian columns and collapsing columns for continuous discharge where the gas is water. The diagram emphasizes that, under the simple circumstances of the model, a decreasing gas content or a widening vent result in an initial plinian phase followed by the formation of ignimbrite by column collapse.

There are many examples of plinian deposits without associated ignimbrites and ignimbrites without associated plinian deposits. These represent eruptions where the conditions were only appropriate for one style of activity. We emphasize that the eruption models that we have presented are for a continuous discharge and do not take detailed account of interruptions in activity. In practice, explosive eruptions are probably not truly continuous but are pulse-like with marked fluctuations in velocity and continuity as episodes of large-clast accumulation and removal occur in the way discussed in Section 6. In addition activity may temporarily cease due to blockage of the vent caused by sudden collapse of the walls or by tectonic movements. Thus there are a number of circumstances which can produce a reinstatement of plinian activity once collapse has begun. There are also eruption sequences (for example the Rio Caliente ignimbrite, Mexico, ignimbrite J, Tenerife and the Roseau Tuff, Dominica) where plinian deposits are found interstratified with ignimbrite flow units. Mechanisms to produce such complex sequences and alternations include a large increase in gas content, increasing proportions of low molecular weight volatiles, sudden closure of the conduit by faulting (see Fig. 13) and relocation of the vent. Choking of the vent by wall collapse may also produce alternations of one style of activity with another, especially if the conditions are close to those at which the transition occurs from convection to collapse.

8 Conclusions

An eruption may be initiated by the opening of a pathway to the surface either as a result of a tensional tectonic event or due to the build-up of an excess pressure in a magma body when gas exsolves from a supersaturated magma. In either case, localization of the eruption pathway may cause the geometry to change from that of a fissure to that of a conduit. If the

fissure or conduit is kept open by tension, the pressure in magma rising through it must be close to lithostatic to avoid wall bursting. If an excess pressure in the magma is responsible for the initiation, the eruption will only proceed with a super-lithostatic pressure gradient until the excess pressure has been relieved. It may then stop as the fissure closes, or, if there is no net tectonic compression in the region, it may continue steadily, being driven at depth by the density contrast between the magma and the relatively denser crustal rocks. In either case, regional subsidence of some sort is needed to replace the erupted magma.

During such adjustment, episodes of conduit restriction may occur as a result of inward faulting of parts of the conduit wall: Fig. 13. These episodes can lead to periods of reduction of mass eruption rate, which otherwise increases with time as conduit erosion occurs. This increase produces a corresponding increase in eruption column height and reverse grading in the air-fall deposit: Fig. 15. This trend can only be significantly modified if magma gas content decreases substantially with time. If vent erosion continues long enough, column collapse always occurs eventually with a change over from air-fall to ash-flow activity. The combinations of values of vent radius (or mass eruption rate) and magma gas content (or eruption velocity) at which collapse occurs for an exit pressure of 1 bar are shown in Fig. 16. Once collapse has occurred, an episode of substantial vent closure and reduction in mass eruption rate is needed to reinstate a plinian column: Fig. 14.

Adjustments in the shape of the upper part of the conduit and lower part of the vent region at depths of the order of hundreds of metres can occur rapidly, especially early in the eruption, as a result of wall bursting: Fig. 3. Nearer the surface, a combination of the expulsion of low-strength materials and deposition of erupted pumice around the vent leads to an outward-flared shape in which the flow can become supersonic (Fig. 4) not far above the level at which magma fragments. Eruption velocities up to 600 m s^{-1} are possible for magmas with total dissolved water contents up to 7 wt per cent and exit pressures of 1 bar, confirming the calculations of McGetchin & Ullrich (1973) for flow in diatremes. As long as exit pressure stays close to 1 bar, eruption velocity is much more strongly dependent on magma gas content than on any other variable: Fig. 6; though the presence of a significant amount of CO_2 in the gas produces a reduction in eruption velocity: Fig. 11. Vent radius depends strongly on both gas content and mass eruption rate: Fig. 7. Mass eruption rate is in turn determined by magma viscosity and by the width of the conduit at depth: equation (24).

In studies of the distribution of large pumice and lithic blocks near vents, velocities of between 350 and 650 m s^{-1} have been deduced (Wilson 1976) for plinian eruptions if the gas phase is water. These velocities imply magmatic water contents of 4–8 per cent and, consequently, minimum depths of magma reservoirs of about 3–12 km.

Fluctuations of a quasi-periodic nature can occur in the exit pressure and velocity as a result of the steady accumulation and occasional expulsion of large clasts in the vent region above the level of magma fragmentation: Fig. 12. While large clasts are present, exit pressure is higher and eruption velocity is smaller, for a given magma gas content and mass eruption rate, than normal. Pressures may rise to several tens of bars if lithic blocks of diameter several metres are present. Such conditions are similar to those which exist if the vent is formed in sufficiently strong surface rocks that no outward flare develops and exit velocities are limited to sonic values. Although lower than when a supersonic transition does occur, exit velocities are still controlled largely by magma gas content (Fig. 8) and vent diameters are related to mass eruption rate (Fig. 9). Exit pressures depend strongly on both gas content and mass eruption rate: Fig. 10.

When the gas exit pressure is greater than 1 bar, a rapid adjustment must take place in the shape of the eruption column just above the vent as it decompresses to 1 bar. The vertical

velocity and width must both increase over a distance scale of a few hundred metres. Thus the distribution of large pumice and lithic clasts within one or two hundred metres of the vent will change during phases of high gas exit pressure. The distribution over the next several hundred metres, out to about 1 or 2 km, will depend on the velocity in the eruption column (Wilson 1976) after it has decompressed to 1 bar, and hence on the magma gas content. In the remainder of the deposit, clast size distribution will depend on the velocity variation in the upper, convective part of the eruption column (Wilson 1976) and on the column height, in turn controlled by the mass eruption rate (Wilson *et al.* 1978).

Acknowledgments

We acknowledge support for parts of this work, performed at the Graduate School of Oceanography, University of Rhode Island, Kingston, R.I. 02881, from the N.S.F. under grants EAR 76-22319 (LW) and OCE 74-22347-A03 (RSJS). RSJS was also supported in part by a NATO Fellowship and LW acknowledges support from the Geological Sciences Department, Brown University, Providence, R.I. 02912, under grant NGR 40-002-116 from the NASA Planetology Program Office. We thank many of our immediate colleagues for stimulating discussions and an anonymous reviewer for valuable comments. This paper is Contribution No. 50 of the Department of Earth Sciences, University of Cambridge.

References

Almond, D. C., 1971. Ignimbrite vents in the Sabaloka Couldron, Sudan, *Geol. Mag.*, **108**, 159–176.

Bennett, F. D., 1974. On volcanic ash formation, *Am. J. Sci.*, **274**, 648–661.

Blackburn, E. A., 1977. Explosive volcanic processes on the Earth and Planets, *PhD thesis*, University of Lancaster.

Bloomfield, K., Sanchez Rubio, G. & Wilson, L., 1977. Plinian eruptions of Nevado de Toluca Volcano, Mexico, *Geol. Rundschau*, **66**, 120–146.

Bond, A. & Sparks, R. S. J., 1976. The Minoan eruption of Santorini, Greece, *J. geol. Soc. Lond.*, **132**, 1–16.

Booth, B., 1973. The Granadilla pumice deposit of Southern Tenerife, Canary Islands, *Proc. geol. Assoc.*, **84**, 353–370.

Cole, B. N., Bowers, H. M. & Hobbs, F., 1969. A theory for the high-speed flow of gas–solids mixtures under conditions of equilibrium and constant frictional lag, in Fluid mechanics and measurements in two phase flow systems, *Proc. Inst. Mech. Engrs*, **184**, 3c, 59–66.

Duffield, W. A., Bacon, C. R. & Roquemore, G. R., 1979. Origin of reverse-graded bedding in air-fall pumice, Coso Range, California, *J. Volcanol. geotherm. Res.*, **5**, 35–48.

Eichelberger, J. C. & Koch, F. G., 1979. Lithic fragments in the Bandelier Tuff, Jemez Mountains, New Mexico, *J. Volcanol. geotherm. Res.*, **5**, 115–134.

Ekren, E. B. & Byers, F. M. Jr, 1976. Ash-flow fissure vent in west-central Nevada, *Geology*, **4**, 247–251.

Heiken, G., 1972. Morphology and petrography of volcanic ashes, *Geol. Soc. Am. Bull.*, **83**, 1961–1988.

Holloway, J. R., 1976. Fluids in the evolution of granitic magmas: Consequences of finite CO_2 solubility, *Geol. Soc. Am. Bull.*, 87, 1513–1518.

Housley, R. M., 1978. Modelling lunar eruptions, *Proc. 9th Lunar planet. Sci. Conf.*, 1473–1484.

Hughes, W. F. & Brighton, J. A., 1967. *Fluid Dynamics*, Schaum's Outline Series, McGraw-Hill, New York.

Kieffer, S. W., 1977. Sound speed in liquid-gas mixtures; water–air and water–steam, *J. geophys. Res.*, **82**, 2895–2904.

Kliegel, J. R., 1963. Gas particle nozzle flows, *Ninth (International) Symposium on Combustion*, pp. 811–826, Academic Press, New York.

Kuno, H., Ishikawa, T., Katsui, Y., Yago, Y., Yamasaki, M. & Taneda, S., 1964. Sorting of pumice and lithic fragments as a key to eruptive and emplacement mechanism, *Jap. J. Geol. Geogr.*, **35**, 223–238.

Lirer, L., Pescatore, T., Booth, B. & Walker, G. P. L., 1973. Two Plinian pumice-fall deposits from Somma, Vesuvius, Italy, *Geol. Soc. Am. Bull.*, **84**, 759–772.

McBirney, A. R., 1973. Factors governing the intensity of explosive andesitic eruptions, *Bull. volc.*, **37**, 443–453.

McGetchin, T. R. & Ullrich, W. G., 1973. Xenoliths in maars and diatremes with inferences for the Moon, Mars and Venus, *J. geophys. Res.*, **78**, 1833–1853.

Minakami, T., 1950. On explosive activities of andesitic volcanoes and their forerunning phenomena, *Bull. volc.*, **10**, 59–87.

Pai, S. I., Hsu, Y. & O'Keefe, J. A., 1978. Similar explosive eruptions of lunar and terrestrial volcanoes, *Proc. 9th Lunar planet. Sci. Conf.*, 1485–1508.

Schlichting, H., 1968. *Boundary Layer Theory*, 6th edn, McGraw-Hill, New York.

Self, S., 1976. The recent volcanology of Terceira, Azores, *J. geol. Soc. Lond.*, **132**, 645–666.

Settle, M., 1978. Volcanic eruption clouds and the thermal power output of explosive eruptions, *J. Volcanol. geotherm. Res.*, **3**, 309–324.

Shaw, H. R., 1963. Obsidian – H_2O viscosities at 1000 and 2000 bars in the temperature range 700°C to 900°C, *J. geophys. Res.*, **68**, 6337–6343.

Shaw, H. R., 1974. Diffusion of H_2O in granitic liquids; Part I. Experimental data; Part II. Mass transfer in magma chambers, in *Geochemical Transport and Kinetics*, pp. 139–170, Carnegie Institution Publication, Washington.

Smith, R. L., 1979. Ash-flow magmatism, *Geol. Soc. Am. Special Paper 180*, eds Chapin, C. E. & Elston, W. E., 5–27.

Sommer, M. A., 1977. Volatiles H_2O, CO_2 and CO in silicate melt inclusions in quartz phenocrysts from the rhyolitic Bandelier Air-fall and Ash-flow tuff, *J. Geol.*, **85**, 423–432.

Soo, S. L., 1961. Gas dynamic processes involving suspended solids, *Am. Inst. chem. Engng J.*, **7**, 384–391.

Soo, S. L., 1967. *Fluid Dynamics of Multiphase Systems*, Blaisdell, Waltham, Massachusetts.

Sparks, R. S. J., 1978. The dynamics of bubble formation in magmas: a review and analysis, *J. Volcanol. geotherm. Res.*, **3**, 1–37.

Sparks, R. S. J. & Wilson, L., 1976. A model for the formation of ignimbrite by gravitational column collapse, *J. geol. Soc. Lond.*, **132**, 441–451.

Sparks, R. S. J., Wilson, L. & Hulme, G., 1978. Theoretical modelling of the generation, movement and emplacement of pyroclastic flows by column collapse, *J. geophys. Res.*, **83**, 1727–1739.

Sparks, R. S. J., Wilson, L. & Sigurdsson, H., 1980. The pyroclastic deposits of the 1875 eruption of Askja, Iceland, *Phil. Trans. R. Soc. Lond. A*, in press.

Steinberg, G. S. & Steinberg, A. S., 1975. On possible causes of volcanic tremors, *J. geophys. Res.*, **80**, 1600–1604.

Taniguchi, H., 1974. The study of the physical and chemical properties of some volcanic acid glasses, *Sci. Rpts Tohoku University*, series III, Vol. XII (2), 189–237.

Tuttle, O. S. & Bowen, N. L., 1958. Origin of granite in the light of experimental studies in the system $NaAlSi_3O_8$–$KAlSi_3O_8$–SiO_2–H_2O, *Geol. Soc. Am. Mem.*, **74**, 1–153.

Walker, G. P. L., 1972. Crystal concentration in ignimbrites, *Contr. Mineral. Petrol.*, **36**, 135–146.

Walker, G. P. L., 1973. Explosive volcanic eruptions; a new classification scheme, *Geol. Rundschau*, **62**, 431–446.

Walker, G. P. L. & Croasdale, R., 1971. Two plinian-type eruptions in the Azores, *J. geol. Soc. Lond.*, **127**, 17–55.

Walker, G. P. L., Wilson, L. & Bowell, E. L. G., 1971. Explosive volcanic eruptions – I. The rate of fall of pyroclasts, *Geophys. J. R. astr. Soc.*, **22**, 377–383.

Walker, G. P. L., 1980. The Taupo pumice, product of the most powerful known (ultraplinian) eruption? *J. Volcanol. geotherm. Res.*, in press.

Wilson, L., 1976. Explosive Volcanic Eruptions – III. Plinian Eruption Columns, *Geophys. J. R. astr. Soc.*, **45**, 543–556.

Wilson, L., 1978. Energetics of the Minoan Eruption, in *Thera and the Aegean World, Proc. 2nd Int. Conf.*, pp. 221–228, ed. Doumas, C.

Wilson, L., Sparks, R. S. J., Huang, T. C. & Watkins, N. D., 1978. The control of eruption column heights by eruption energetics and dynamics, *J. geophys. Res.*, **83**, 1829–1836.